Journal of Computational and Applied Mathematics 436 (2024) 115422

Contents lists available at ScienceDirect

Journal of Computational and Applied Mathematics

journal homepage: www.elsevier.com/locate/cam

A numerical approach for a two-parameter singularly perturbed weakly-coupled system of 2-D elliptic convection–reaction–diffusion PDEs

Carmelo Clavero [a,*], Ram Shiromani [b], Vembu Shanthi [b]

[a] Department of Applied Mathematics, IUMA, University of Zaragoza, Zaragoza, Spain
[b] Department of Mathematics, National Institute of Technology, Tiruchirappalli, Tamilnadu, India

ARTICLE INFO

Article history:
Received 2 December 2022
Received in revised form 16 March 2023

MSC:
35J25
35J40
35B25
65N06
65N12
65N15
65N50

Keywords:
Convection and source terms
Finite difference scheme
Bakhvalov–Shishkin mesh
Elliptic coupled system
Two parameter singularly perturbed problem
Two dimensional space

ABSTRACT

In this work, we consider the numerical approximation of a two dimensional elliptic singularly perturbed weakly-coupled system of convection–reaction–diffusion type, which has two different parameters affecting the diffusion and the convection terms, respectively. The solution of such problems has, in general, exponential boundary layers as well as corner layers. To solve the continuous problem, we construct a numerical method which uses a finite difference scheme defined on an appropriate layer-adapted Bakhvalov–Shishkin mesh. Then, the numerical scheme is a first order uniformly convergent method with respect both convection and diffusion parameters. Numerical results obtained with the algorithm for some test problems are presented, which show the best performance of the proposed method, and they also corroborate in practice the theoretical analysis.

1. Introduction

Singularly perturbed systems are a good model for different physical phenomena, as reaction–diffusion enzyme model, saturated flow in fractured porous media, tubular model in chemical reactor theory, combustion process, diffusion process in electro-analytic chemistry or neutron transport model (see by instance [1–5]). In general, the solution of these problems has boundary layers and/or internal layers, depending of the coefficients in the differential equation and/or in the boundary conditions, which appear near the boundary or at the interior of the domain; in those regions, the exact solution has extremely higher gradients. So, appropriate numerical methods are needed to find a good approximate solution in the domain where the problem is defined. Then, uniformly convergent methods are necessary, i.e., methods for which the numerical approximation is adequate independently of the value of both positive convection and diffusion parameters, which can be very small.

Problems having two small parameters in the differential equation, affecting to the convection and the diffusion terms, are interesting in the context of the singular perturbation problems. For instance, in [6,7], the case of one elliptic scalar

* Corresponding author.
E-mail addresses: clavero@unizar.es (C. Clavero), ram.panday.786@gmail.com (R. Shiromani), vshanthi@nitt.edu (V. Shanthi).

https://doi.org/10.1016/j.cam.2023.115422

equation was considered and efficient numerical method was developed to solve this type of problems. More recently, in [8–10], one dimensional parabolic scalar problems, having also a delay term in the differential equation, were analyzed. In all those works, the numerical method combines the implicit Euler method to discretize in time, on a uniform mesh, together with the classical upwind scheme to discretize in space on some special nonuniform meshes of Shishkin type, which includes the Shishkin, the Bakhvalov–Shishkin and the Duran–Shishkin meshes; it was proved that the fully discrete method is uniformly convergent with respect both small parameters, and also that the use of the Bakhvalov–Shishkin mesh gives better numerical results that when the Shishkin mesh is used.

In the literature, there are many works where adequate numerical methods have been constructed for solving elliptic or parabolic singularly perturbed coupled systems, for one or two dimensional problems in space, so much for reaction–diffusion as convection–reaction–diffusion problems. In [11–14], 1D convection–diffusion elliptic systems were analyzed. In [15,16], and elliptic 2D system of reaction–diffusion and convection–diffusion type, respectively, was considered. In [17–20] parabolic one dimensional weakly coupled systems of convection–diffusion type, with equal or different diffusion parameters were solved. In [21,22] parabolic two dimensional weakly coupled systems of convection–diffusion type, for which the diffusion parameter is the same in both equations of the system, were studied. In all previous papers, uniformly convergent numerical methods were constructed to solve the corresponding singularly perturbed problems.

A different and considerably more complex problem appears when in the coupled system there are two small parameters affecting to both the diffusion and the convection terms. So far, we only know the work [23] for that type problems; in that work, a parabolic one dimensional weakly coupled system of convection–diffusion type, which has a discontinuity in the source term and small parameters at both the diffusion and the convection terms, was considered; then, combining the implicit Euler method to discretize in time, on a uniform mesh and the upwind scheme to discretize in space, on a piecewise uniform Shishkin mesh, the resulting fully discrete scheme is an almost first order uniformly convergent method. Nevertheless, up to our knowledge, there are not any work where a elliptic two dimensional weakly coupled system of convection–diffusion type, with small parameters at both the diffusion and the convection terms, is considered.

In this paper, we are interested in solving this type of coupled systems by using a upwind scheme to discretize in space, which is defined on a special nonuniform Bakhvalov–Shishkin mesh. Concretely, we consider a two-parameter singularly perturbed weakly-coupled system of 2-D elliptic convection–reaction–diffusion equation, given by

$$\begin{cases} \mathcal{L}_{\varepsilon,\mu}\vec{\mathbf{z}}(x,y) \equiv \varepsilon\left(\dfrac{\partial^2\vec{\mathbf{z}}}{\partial x^2}+\dfrac{\partial^2\vec{\mathbf{z}}}{\partial y^2}\right)+\mu\left(\vec{\mathbf{A}}(x,y)\dfrac{\partial\vec{\mathbf{z}}}{\partial x}+\vec{\mathbf{B}}(x,y)\dfrac{\partial\vec{\mathbf{z}}}{\partial y}\right)-\vec{\mathbf{C}}(x,y)\vec{\mathbf{z}}=\vec{\mathbf{f}}(x,y), \quad \forall(x,y)\in\Omega, \\ \vec{\mathbf{z}}(x,y)=\vec{\mathbf{g}}(x,y), \quad \forall(x,y)\in\partial\Omega, \end{cases} \tag{1.1}$$

where

$$\Omega=(0,1)\times(0,1),\ \vec{\mathbf{z}}(x,y)=(z_1(x,y),z_2(x,y))^T,\ \vec{\mathbf{f}}(x,y)=(f_1(x,y),f_2(x,y))^T,\ \vec{\mathbf{g}}(x,y)=(g_{i1}(x,y),g_{i2}(x,y))^T,$$
$$i=1,2,3,4,\ \vec{\mathbf{A}}(x,y)=\begin{pmatrix} a_1(x,y) & 0\\ 0 & a_2(x,y)\end{pmatrix},\ \vec{\mathbf{B}}(x,y)=\begin{pmatrix} b_1(x,y) & 0\\ 0 & b_2(x,y)\end{pmatrix},\ \vec{\mathbf{C}}(x,y)=\begin{pmatrix} c_{11}(x,y) & c_{12}(x,y)\\ c_{21}(x,y) & c_{22}(x,y)\end{pmatrix}.$$

The two small perturbation parameters satisfy $0<\epsilon,\mu\ll 1$. We assume that the convection and reaction terms satisfy

$$\begin{cases} a_i(x,y)\geq\alpha_1>0,\ b_i(x,y)\geq\alpha_2>0,\ i=1,2,\\ (c_{i1}(x,y)-c_{i2}(x,y))\geq\beta>0,\ c_{ii}(x,y)>0,\ i=1,2,\\ c_{ii}(x,y)>|c_{ij}(x,y)|, \quad i,j=1,2,\ i\neq j, \end{cases} \tag{1.2}$$

for some positive constants α_1, α_2 and β. Let be

$$\alpha=\min(\alpha_1,\alpha_2),\ \lambda=\min_{i,j}\left\{\frac{c_{ii}-c_{ij}}{2a_i},\frac{c_{ii}-c_{ij}}{2b_i}\right\},\ \text{for } i,j=1,2,\ i\neq j. \tag{1.3}$$

We will also assume that the components of $\vec{\mathbf{A}}$, $\vec{\mathbf{B}}$, $\vec{\mathbf{f}}$ and $\vec{\mathbf{C}}$ are sufficiently smooth on the domain Ω, $\vec{\mathbf{g}}\in C^{4,\gamma}(\partial\Omega)$, for some $\gamma\in(0,1]$, and they satisfy sufficient compatibility conditions in order that the continuous problem has an unique solution $\vec{\mathbf{z}}$ such that $\vec{\mathbf{z}}\in C^{4,\gamma}(\Omega)$. (see [24,25], Theorem 3.2).

We denote the four sides of Ω by

$$\partial\Omega=\begin{cases} \Lambda_1=\{(0,y)\mid(0\leq y\leq 1)\}, & \Lambda_2=\{(x,0)\mid(0\leq x\leq 1)\},\\ \Lambda_3=\{(1,y)\mid(0\leq y\leq 1)\}, & \Lambda_4=\{(x,1)\mid(0\leq x\leq 1)\}, \end{cases}$$

and $\Lambda=\Lambda_1\cup\Lambda_2\cup\Lambda_3\cup\Lambda_4$. Recalling from (1.1) that $\vec{\mathbf{z}}=\vec{\mathbf{g}}$ on the boundary, we denote by $\vec{\mathbf{g}}_i$, $i=1,2,3,4$, the restriction of $\vec{\mathbf{g}}$ onto Λ_i, $i=1,2,3,4$.

Following [26], we write the compatibility conditions at the corner point $(0,0)$, for the first equation of the coupled system; similarly can be made for the other three corners and the second equation of the system. We denote $g_1(y)=$

$g_{11}(0, y)$, $g_2(x) = g_{21}(x, 0)$ and $g_3(y) = g_{12}(0, y)$. To short, we only write the compatibility conditions up to second order, but in the same way that in [26], higher order compatibility conditions can be given. These conditions are

$$g_1(0) = g_2(0),$$
$$-\varepsilon(g_2''(0) + g_1''(0)) + \mu(a_1(0, 0)g_2'(0) + b_1(0, 0)g_1'(0)) - c_{11}(0, 0)g_1(0) - c_{12}(0, 0)g_3(0) = f_1(0, 0).$$

The paper is structured as follows. In Section 2, we prove a minimum principle for the continuous problem, we establish a stability result and we also give appropriate estimates for the exact solution and its derivatives, from which it follows their dependence on both singular perturbation parameters ε and μ. In Section 3, we define the numerical approach by using the standard 5-point finite difference scheme built on a Shishkin-type mesh. In Section 4, we prove estimates for the error; from them, if follows that the scheme is a first-order uniformly convergent method on a Bahkvalov–Shishkin mesh. In Section 5, some test problems are solved to corroborate in practice the theoretical results. Finally, in Section 6, some conclusions are given.

Henceforth, we denote by $\|\cdot\|$ the continuous maximum norm; moreover, C denotes a generic positive constant which is independent of the diffusion parameter ε, the convection parameter μ and the discretization parameter N.

2. Asymptotic behavior of the exact solution

The present section contains the continuous minimum principle, a stability result and some useful bounds for the derivatives of the exact solution of the continuous problem (1.1). In addition, we obtain some appropriate bounds for the regular, singular and corner components of the solution, which are defined below.

We follow the approach in ([23], Lemma 2.2), where a parabolic 1D system with two parameters was considered, to prove a continuous minimum principle for problem (1.1), where an elliptic 2D system with two parameters is considered.

Lemma 2.1 (*Minimum Principle*)**.** *Let $\mathcal{L}_{\epsilon,\mu}$ be the differential operator given in (1.1) and we assume that (1.2) holds. If $\vec{\boldsymbol{\phi}}(x, y) \geq \vec{\mathbf{0}}$ on $\partial\Omega$, $\mathcal{L}_{\varepsilon,\mu}\vec{\boldsymbol{\phi}}(x, y) \leq \vec{\mathbf{0}}$ for all $(x, y) \in \Omega$, and there exists a function $\vec{\boldsymbol{\nu}} = (\nu_1, \nu_2)$ satisfying $\vec{\mathbf{v}}(x, y) > \vec{\mathbf{0}}$ on $\partial\Omega$, and $\mathcal{L}_{\varepsilon,\mu}\vec{\mathbf{v}}(x, y) \leq \vec{\mathbf{0}}$ for all $(x, y) \in \Omega$, then it holds $\vec{\boldsymbol{\phi}}(x, y) \geq \vec{\mathbf{0}}$ for all $(x, y) \in \bar{\Omega}$.*

Proof. We consider the functions

$$\Psi_1 = \max_{(x,y)\in\bar{\Omega}}\left(-\frac{\phi_1}{\nu_1}\right)(x, y), \quad \Psi_2 = \max_{(x,y)\in\bar{\Omega}}\left(-\frac{\phi_2}{\nu_2}\right)(x, y),$$

and we denote $\Psi = \max\{\Psi_1, \Psi_2\}$. Let be $\mathcal{L}_{\varepsilon,\mu} = (\mathcal{L}^1_{\varepsilon,\mu}, \mathcal{L}^2_{\varepsilon,\mu})^T$.

Let be $\vec{\boldsymbol{\phi}}(x^*, y^*) = \min_{(x,y)\in\bar{\Omega}}\{\vec{\boldsymbol{\phi}}(x, y)\}$. If $\vec{\boldsymbol{\phi}}(x^*, y^*) \geq \vec{\mathbf{0}}$, there is nothing to prove. Suppose $\vec{\boldsymbol{\phi}}(x^*, y^*) < \vec{\mathbf{0}}$ implies that $\Psi(x, y) > 0$. Then, by the assumption on the boundary values, the point $(x^*, y^*) \in \Omega$ for which $\Psi_1 = \Psi$ or $\Psi_2 = \Psi$ or $\Psi_1 = \Psi_2 = \Psi$ and $(\vec{\boldsymbol{\phi}} + \Psi\vec{\mathbf{v}})(x, y) \geq 0$, $\forall(x, y) \in \bar{\Omega}$.

Let us consider the point $(x^*, y^*) \in \Omega$ and $\Psi_1 = \left(-\frac{\phi_1}{\nu_1}\right)(x^*, y^*) = \Psi$ and $(\phi_1 + \Psi\nu_1)(x^*, y^*) = 0$. This exhibits that $(\phi_1 + \Psi\nu_1)$ having minimum at the point $(x, y) = (x^*, y^*)$. We have

$$\mathcal{L}^1_{\varepsilon,\mu}(\phi_1 + \Psi\nu_1)(x^*, y^*) = \varepsilon\left(\frac{\partial^2}{\partial x^2} + \frac{\partial^2}{\partial y^2}\right)(\phi_1 + \Psi\nu_1)(x^*, y^*) + \mu\left(a_1\frac{\partial}{\partial x} + b_1\frac{\partial}{\partial y}\right)(\phi_1 + \Psi\nu_1)(x^*, y^*)$$
$$- c_{11}(x^*, y^*)(\phi_1 + \Psi\nu_1)(x^*, y^*) - c_{12}(x^*, y^*)(\phi_1 + \Psi\nu_1)(x^*, y^*) \geq 0,$$

which contradicts the hypothesis. Similarly, we can prove the contradiction if we choose $\Psi_2 = \left(-\frac{\phi_2}{\nu_2}\right)(x^*, y^*) = \Psi$. This completes the proof. □

A consequence of this minimum principle is the parameter uniform boundedness of the solution of (1.1) given below.

Lemma 2.2 (*Stability Result*)**.** *Let $\vec{\mathbf{z}}(x, y)$ be the solution of (1.1) and we assume that (1.2) holds. Then, we have*

$$\|\vec{\mathbf{z}}(x, y)\|_{\bar{\Omega}} \leq \frac{1}{\alpha}\|\mathcal{L}_{\varepsilon,\mu}\vec{\mathbf{z}}\|_{\bar{\Omega}} + \max\left\{\|\vec{\mathbf{z}}\|_{\Lambda_1}, \|\vec{\mathbf{z}}\|_{\Lambda_2}, \|\vec{\mathbf{z}}\|_{\Lambda_3}, \|\vec{\mathbf{z}}\|_{\Lambda_4}\right\},$$

where α is defined in (1.3).

Proof. We define the barrier functions

$$\vec{\boldsymbol{\Phi}}^{\pm}(x, y) = \frac{1}{\alpha}\|\mathcal{L}_{\varepsilon,\mu}\vec{\mathbf{z}}\|_{\bar{\Omega}} + \max\left\{\|\vec{\mathbf{z}}\|_{\Lambda_1}, \|\vec{\mathbf{z}}\|_{\Lambda_2}, \|\vec{\mathbf{z}}\|_{\Lambda_3}, \|\vec{\mathbf{z}}\|_{\Lambda_4}\right\} \pm \vec{\mathbf{z}}(x, y),$$

and with the help of Lemma 2.1 we can get the required result. □

For the posterior analysis of the uniform convergence of the numerical method, we need appropriate estimates of the derivatives of the exact solution; these estimates depends, of course, of the parameters ε and μ and also on the ratio between them, because the nature of the exact solution change depending on this ratio. The first step to deduce those estimates, is the following result, which gives vast estimates for derivatives.

Lemma 2.3. *Let $\vec{\mathbf{z}} = (z_1, z_2)^T$ be the solution of continuous problem (1.1) and we assume that (1.2) holds. Then, for $1 \le i+j \le 4$, it holds*

*(**i**) If $\alpha\mu^2 \le \lambda\varepsilon$, then*

$$\left\| \frac{\partial^{i+j}\vec{\mathbf{z}}}{\partial x^i \partial y^j} \right\|_{\Omega} \le C\varepsilon^{-(i+j)/2}, \tag{2.1}$$

*(**ii**) If $\alpha\mu^2 > \lambda\varepsilon$, then*

$$\left\| \frac{\partial^{i+j}\vec{\mathbf{z}}}{\partial x^i \partial y^j} \right\|_{\Omega} \le C\left(\frac{\varepsilon}{\mu}\right)^{-(i+j)}, \tag{2.2}$$

where λ is defined in (1.3) and C is a positive constant independent of ε and μ.

Proof. We follow the standard procedures given in [24,27]. The bounds of the solution and its derivatives can be obtained by splitting the arguments into two cases: $\alpha\mu^2 \le \lambda\varepsilon$ and $\alpha\mu^2 > \lambda\varepsilon$.
Case 1: If $\alpha\mu^2 \le \lambda\varepsilon$. Now, we consider the transforming variables $\zeta = x/\sqrt{\varepsilon}$, $\xi = y/\sqrt{\varepsilon}$. The transformed domain is given by $\Omega^* = (0, 1/\sqrt{\varepsilon})^2$. On the domain Ω^*, the transformed functions are defined as $\vec{\mathbf{z}}^*(\zeta,\xi) = \vec{\mathbf{z}}(x,y)$, $\vec{\mathbf{A}}^*(\zeta,\xi) = \vec{\mathbf{A}}(x,y)$, $\vec{\mathbf{B}}^*(\zeta,\xi) = \vec{\mathbf{f}}^*(\zeta,\xi) = \vec{\vec{\mathbf{z}}}^*(\zeta,\xi)$. Now, we denote the rectangle $\mathfrak{A}_{\kappa^*,\upsilon^*} = (\kappa^* - \upsilon^*, \kappa^* + \upsilon^*)^2 \cap \Omega^*$, and $\overline{\mathfrak{A}}_{\kappa^*,\upsilon^*}$ is the closure of $\mathfrak{A}_{\kappa^*,\upsilon^*}$, where $\}\kappa^* \in \Omega^*$ and $\upsilon^* > 0$. For every (κ^*, υ^*), the above classical differential equation holds the following estimate for $1 \le i+j \le 4$:

$$\left\| \frac{\partial^{i+j}\vec{\mathbf{z}}}{\partial \zeta^i \partial \xi^j} \right\|_{\mathfrak{A}_{\kappa^*,\upsilon^*}} \le C.$$

Hence, these estimate holds for any point $(\zeta,\xi) \in \Omega^*$ and therefore, in the original variables (x,y), (2.1) follows.
Case 2: If $\alpha\mu^2 > \lambda\varepsilon$. Now, we consider the two stretched variables $\Upsilon = \mu x/\varepsilon$, $\varphi = \mu y/\varepsilon$. The transformed domain now is given by $\Omega^{**} = (0, \mu/\varepsilon)^2$. On the domain Ω^{**}, the stretched functions are defined as $\vec{\mathbf{z}}^{**}(\Upsilon,\varphi) = \vec{\mathbf{z}}(x,y)$, $\vec{\mathbf{A}}^{**}(\Upsilon,\varphi) = \vec{\mathbf{A}}(x,y)$, $\vec{\mathbf{B}}^{**}(\Upsilon,\varphi) = \vec{\mathbf{B}}(x,y)$, $\vec{\mathbf{C}}^{**}(\Upsilon,\varphi) = \vec{\mathbf{C}}(x,y)$ and $\vec{\mathbf{f}}^{**}(\Upsilon,\varphi) = \vec{\mathbf{f}}(x,y)$. We apply the above transformation for the governing problem (1.1); from this transformed equation we get the solution $\vec{\mathbf{z}}^{**}(\Upsilon,\varphi)$. Again, we denote the rectangle $\mathfrak{A}_{\kappa^{**},\upsilon^{**}} = (\kappa^{**} - \upsilon^{**}, \kappa^{**} + \upsilon^{**})^2 \cap \Omega^{**}$, and $\overline{\mathfrak{A}}_{\kappa^{**},\upsilon^{**}}$ is the closure of $\mathfrak{A}_{\kappa^{**},\upsilon^{**}}$, where $\kappa^{**} \in \Omega^{**}$ and $\upsilon^{**} > 0$. For every $(\kappa^{**}, \upsilon^{**})$, the above classical differential equation holds the following estimate for $1 \le i+j \le 4$:

$$\kappa^{**}, \upsilon^{**} \le C.$$

Hence, these estimate holds for any point $(\Upsilon,\varphi) \in \Omega^{**}$ and therefore, in the original variables (x,y), (2.2) follows. □

Previous bounds are not adequate to prove posteriorly the uniform convergence of the numerical method, because they do not reflect the existence of boundary and internal layers in the exact solution of (1.1). To obtain good estimates, we follow a usual technique in the context of singular perturbation problems. Then, we decompose the continuous solution $\vec{\mathbf{z}}(x,y)$ into the three components, $\vec{\mathbf{z}} = \vec{\mathbf{r}} + \vec{\mathbf{w}} + \vec{\mathbf{s}}$. The first component is the smooth component (non-layer); the second and third components are the boundary and corner layer components, respectively, which can be split into $\vec{\mathbf{w}}_b$, $\vec{\mathbf{w}}_t$, $\vec{\mathbf{w}}_l$, $\vec{\mathbf{w}}_r$ and $\vec{\mathbf{s}}_{lb}$, $\vec{\mathbf{s}}_{br}$, $\vec{\mathbf{s}}_{rt}$, $\vec{\mathbf{s}}_{lt}$, respectively.

The smooth component $\vec{\mathbf{r}}(x,y)$ is obtained as the solution of the problem

$$\begin{cases} \mathcal{L}_{\varepsilon,\mu}\vec{\mathbf{r}}(x,y) = \vec{\mathbf{f}}(x,y), \ \ \forall (x,y) \in \Omega, \\ \vec{\mathbf{r}}(x,y) = \vec{\mathbf{g}}_1(y), \quad \forall (x,y) \in \Lambda_1, \quad \vec{\mathbf{r}}(x,y) = \vec{\mathbf{g}}_2(x), \quad \forall (x,y) \in \Lambda_2, \\ \vec{\mathbf{r}}(x,y) = \vec{\mathbf{g}}_3(y), \quad \forall (x,y) \in \Lambda_3, \quad \vec{\mathbf{r}}(x,y) = \vec{\mathbf{g}}_4(x), \quad \forall (x,y) \in \Lambda_4, \end{cases} \tag{2.3}$$

Lemma 2.4. *The smooth component $\vec{\mathbf{r}}(x,y)$ and their derivatives hold the following bounds:*

*(**i**) If $\alpha\mu^2 \le \lambda\varepsilon$, then*

$$\left\| \frac{\partial^{i+j}\vec{\mathbf{r}}}{\partial x^i \partial y^j} \right\|_{\Omega} \le C\left(1 + \varepsilon^{1-(i+j)/2}\right), \qquad \text{for} \quad 1 \le i+j \le 4,$$

*(**ii**) If $\alpha\mu^2 > \lambda\varepsilon$, then*

$$\left\| \frac{\partial^{i+j}\vec{\mathbf{r}}}{\partial x^i \partial y^j} \right\|_{\Omega} \le C\left(1 + \left(\frac{\varepsilon}{\mu}\right)^{2-(i+j)}\right), \quad \text{for} \quad 1 \le i+j \le 4,$$

where λ is defined in (1.3).

Proof. Let us consider separately the two cases.
Case(i): Firstly, we assume that $\alpha\mu^2 \le \lambda\epsilon$ holds. Then, we decompose the smooth component $\vec{\mathbf{r}}(x,y;\varepsilon,\mu)$ as

$$\vec{\mathbf{r}}(x,y) = \vec{\mathbf{r}}_0(x,y,\varepsilon,\mu) + \sqrt{\varepsilon}\vec{\mathbf{r}}_1(x,y,\varepsilon,\mu) + \varepsilon\vec{\mathbf{r}}_2(x,y,\varepsilon,\mu), \tag{2.4}$$

where

$$-\vec{\mathbf{C}}\vec{\mathbf{r}}_0(x,y)=\vec{\mathbf{f}}(x,y),\quad \vec{\mathbf{C}}\vec{\mathbf{r}}_1(x,y)=\sqrt{\varepsilon}\left(\frac{\partial^2}{\partial x^2}+\frac{\partial^2}{\partial y^2}\right)\vec{\mathbf{r}}_0(x,y)+\frac{\mu}{\sqrt{\varepsilon}}\left(\vec{\mathbf{A}}\frac{\partial}{\partial x}+\vec{\mathbf{B}}\frac{\partial}{\partial y}\right)\vec{\mathbf{r}}_0(x,y), \tag{2.5}$$

and

$$\mathcal{L}_{\varepsilon,\mu}\vec{\mathbf{r}}_2=-\sqrt{\varepsilon}\left(\frac{\partial^2}{\partial x^2}+\frac{\partial^2}{\partial y^2}\right)\vec{\mathbf{r}}_1(x,y)-\frac{\mu}{\sqrt{\varepsilon}}\left(\vec{\mathbf{A}}\frac{\partial}{\partial x}+\vec{\mathbf{B}}\frac{\partial}{\partial y}\right)\vec{\mathbf{r}}_1(x,y),\quad \vec{\mathbf{r}}_2=\vec{\mathbf{0}},\ \forall (x,y)\in\Lambda. \tag{2.6}$$

Note that $\vec{\mathbf{r}}_0$ and $\vec{\mathbf{r}}_1$ satisfy zeroth order differential problems (2.5) and therefore there are no issue of compatibility. The term $\vec{\mathbf{r}}_2$ denotes the solution of an elliptic problem on the domain Ω. Since, $\vec{\mathbf{r}}_0\in C^{4,\gamma}(\bar{\Omega})$, we get $\left(\frac{\partial^2}{\partial x^2}+\frac{\partial^2}{\partial y^2}\right)\vec{\mathbf{r}}_0\in C^{2,\gamma}(\bar{\Omega})$.

Applying Lemmas 2.2 and 2.3 to the problem (2.3), it results that $\vec{\mathbf{r}}\in C^{4,\gamma}(\Omega)$ and also that it holds

$$\left\|\frac{\partial^{i+j}\vec{\mathbf{r}}}{\partial x^i\partial y^j}\right\|\le C(1+\epsilon^{1-(i+j)/2}),\quad 1\le i+j\le 4. \tag{2.7}$$

Case(ii): In second place, we assume that $\alpha\mu^2>\lambda\epsilon$ holds. In this case, the smooth component $\vec{\mathbf{r}}(x,y;\varepsilon,\mu)$ can be decomposed as

$$\vec{\mathbf{r}}(x,y;\varepsilon,\mu)=\vec{\mathbf{r}}_0(x,y;\mu)+\varepsilon\vec{\mathbf{r}}_1(x,y;\mu)+\varepsilon^2\vec{\mathbf{r}}_2(x,y;\varepsilon,\mu),$$

where now the functions $\vec{\mathbf{r}}_0$, $\vec{\mathbf{r}}_1$ and $\vec{\mathbf{r}}_2$ are the solutions of the following problems:

$$\mathcal{L}_{\mu}\vec{\mathbf{r}}_0=\vec{\mathbf{f}},\ \vec{\mathbf{r}}_0(x,y)=\vec{\mathbf{z}}(x,y),\ \forall(x,y)\in\Lambda_3\cup\Lambda_4,$$

$$\mathcal{L}_{\mu}\vec{\mathbf{r}}_1=-\left(\frac{\partial^2}{\partial x^2}+\frac{\partial^2}{\partial y^2}\right)\vec{\mathbf{r}}_0,\ \vec{\mathbf{r}}_1(x,y)=\vec{\mathbf{0}},\ \forall(x,y)\in\Lambda_3\cup\Lambda_4,$$

$$\mathcal{L}_{\varepsilon,\mu}\vec{\mathbf{r}}_2=-\left(\frac{\partial^2}{\partial x^2}+\frac{\partial^2}{\partial y^2}\right)\vec{\mathbf{r}}_1,\quad \vec{\mathbf{r}}_2(x,y)=\vec{\mathbf{0}},\ \forall(x,y)\in\Lambda.$$

Applying again Lemmas 2.2 and 2.3 to the problem (2.3) we get

$$\left\|\frac{\partial^{i+j}\vec{\mathbf{r}}}{\partial x^i\partial y^j}\right\|\le C\left(1+\left(\frac{\varepsilon}{\mu}\right)^{2-(i+j)}\right),\quad 1\le i+j\le 4, \tag{2.8}$$

which is the required result. □

Now, let us consider the first order IBVP

$$\mathcal{L}_{\mu}\vec{\mathbf{z}}(x,y)=\mu\left(\vec{\mathbf{A}}(x,y)\frac{\partial\vec{\mathbf{z}}}{\partial x}+\vec{\mathbf{B}}(x,y)\frac{\partial\vec{\mathbf{z}}}{\partial y}\right)-\vec{\mathbf{C}}(x,y)\vec{\mathbf{z}}=\vec{\mathbf{f}}(x,y),\ \forall(x,y)\in\Omega, \tag{2.9a}$$

$$\vec{\mathbf{z}}(x,y)=\vec{\mathbf{g}}_i,\ (x,y)\in\Lambda_i,\ i=3,4. \tag{2.9b}$$

Note that $\mathcal{L}_{\mu}$ satisfies the following comparison principle.

Lemma 2.5. *Let $\mathcal{L}_{\mu}$ be the differential operator given in (2.9). If $\vec{\boldsymbol{\phi}}(x,y)\ge\vec{\mathbf{0}}$ on Λ_i, $i=3,4$, $\mathcal{L}_{\mu}\vec{\boldsymbol{\phi}}(x,y)\le\vec{\mathbf{0}}$ for all $(x,y)\in\Omega$, then it is $\vec{\boldsymbol{\phi}}(x,y)\ge\vec{\mathbf{0}}$ for all $(x,y)\in\bar{\Omega}$.*

Proof. The proof is similar to this one of Lemma 2.1. □

Lemma 2.6. *Let $\vec{\mathbf{z}}(x,y)$ be the solution of problem (2.9). Then, it holds the stability estimate*

$$\|\vec{\mathbf{z}}(x,y)\|_{\bar{\Omega}}\le\frac{1}{\alpha}\|\mathcal{L}_{\mu}\vec{\mathbf{z}}\|_{\Omega}+\max\left\{\|\vec{\mathbf{z}}\|_{\Lambda_3},\|\vec{\mathbf{z}}\|_{\Lambda_4}\right\},$$

where α is defined in (1.3).

Proof. This lemma can be proved similarly to Lemma 2.2. □

Corresponding to the left edge $x=0$ in Ω, a boundary layer component $\vec{\mathbf{w}}_l$ exists that is the solution of the problem

$$\mathcal{L}_{\varepsilon,\mu}\vec{\mathbf{w}}_l=\vec{\mathbf{0}},\quad \forall(x,y)\in\Omega, \tag{2.10a}$$

$$\vec{\mathbf{w}}_l(x,y)=(\vec{\mathbf{z}}-\vec{\mathbf{r}})(x,y),\quad \forall(x,y)\in\Lambda_1, \tag{2.10b}$$

$$\vec{\mathbf{w}}_l(x,y)=\vec{\mathbf{0}},\quad \forall(x,y)\in\Lambda_2\cup\Lambda_3\cup\Lambda_4. \tag{2.10c}$$

The following Lemmas give some bounds on the derivatives of this layer component, which are necessary for the posterior analysis of the uniform convergence of the numerical method.

Lemma 2.7. *Let $\vec{\mathbf{w}}_l$ be the boundary layer component satisfying the equations in (2.10). If $\alpha\mu^2 \le \lambda\varepsilon$, then it holds*

$$|\vec{\mathbf{w}}_l(x,y)| \le C\exp\left(-\sqrt{\frac{\alpha_1\lambda}{\varepsilon}}x\right), \quad \left\|\frac{\partial^j \vec{\mathbf{w}}_l}{\partial y^j}\right\| \le C(1+\epsilon^{(1-j)/2}), \quad j=1,2,3,4. \tag{2.11}$$

On the other hand, if $\alpha\mu^2 > \lambda\varepsilon$, then it holds

$$|\vec{\mathbf{w}}_l(x,y)| \le C\exp\left(-\frac{\alpha_1\mu}{\epsilon}x\right), \quad \left\|\frac{\partial^j \vec{\mathbf{w}}_l}{\partial y^j}\right\| \le C\left(1+\left(\frac{\epsilon}{\mu}\right)^{-j}\right), \quad j=1,2,3,4, \tag{2.12}$$

where λ is defined in (1.3).

Proof. To obtain the bounds for the left boundary layer component $\vec{\mathbf{w}}_l$, we consider the stretched variables $\zeta = \dfrac{x}{\sqrt{\varepsilon}}$ for $\alpha\mu^2 \le \lambda\varepsilon$ and $\Upsilon = \dfrac{\mu x}{\varepsilon}$ for $\alpha\mu^2 > \lambda\varepsilon$; then, the resulting continuous problems after this change of variable, are given by

$$\begin{cases} \left(\dfrac{\partial^2 \vec{\mathbf{w}^*}_l}{\partial\zeta^2} + \varepsilon\dfrac{\partial^2 \vec{\mathbf{w}^*}_l}{\partial y^2}\right) + \mu\varepsilon^{-1/2}\vec{\mathbf{A}^*}(\zeta,y)\dfrac{\partial \vec{\mathbf{w}^*}_l}{\partial\zeta} + \mu\vec{\mathbf{B}^*}(\zeta,y)\dfrac{\partial \vec{\mathbf{w}^*}_l}{\partial y} - \vec{\mathbf{C}^*}(\zeta,y)\vec{\mathbf{w}^*}_l = \vec{\mathbf{f}^*}(\zeta,y), \ \forall(\zeta,y)\in\Omega_\varepsilon^{*,1}, \\ \vec{\mathbf{w}^*}_l(\zeta,y) = (\vec{\mathbf{z}^*} - \vec{\mathbf{r}^*})(\zeta,y), \quad \forall(\zeta,y)\in\Lambda_{1,\varepsilon}^{*,1}, \\ \vec{\mathbf{w}^*}_l(\zeta,y) = \vec{\mathbf{0}}, \quad \forall(\zeta,y)\in\Lambda_{2,\varepsilon}^{*,1}\cup\Lambda_{3,\varepsilon}^{*,1}\cup\Lambda_{4,\varepsilon}^{*,1}, \end{cases} \tag{2.13}$$

in the case that $\alpha\mu^2 \le \lambda\varepsilon$, where $\Omega_\varepsilon^{*,1} = (0,\frac{1}{\sqrt{\varepsilon}})\times(0,1)$ and $\Lambda_{i,\varepsilon}^{*,1}$, $i=1,2,3,4$ are the relative boundaries of the domain $\Omega_\varepsilon^{*,1}$, and by

$$\begin{cases} \left(\varepsilon^{-1}\dfrac{\partial^2 \vec{\mathbf{w}^{**}}_l}{\partial\Upsilon^2} + \varepsilon\mu^{-2}\dfrac{\partial^2 \vec{\mathbf{w}^{**}}_l}{\partial y^2}\right) + \varepsilon^{-1}\vec{\mathbf{A}^{**}}(\Upsilon,y)\dfrac{\partial \vec{\mathbf{w}^{**}}_l}{\partial\Upsilon} + \mu^{-1}\vec{\mathbf{B}^{**}}(\Upsilon,y)\dfrac{\partial \vec{\mathbf{w}^{**}}_l}{\partial y} - \\ \qquad\qquad \mu^{-2}\vec{\mathbf{C}^{**}}(\Upsilon,y)\vec{\mathbf{w}^{**}}_l = \mu^{-2}\vec{\mathbf{f}^{**}}(\Upsilon,y), \ \forall(\Upsilon,y)\in{\Omega^{**}}_\varepsilon^1, \\ \vec{\mathbf{w}^{**}}_l(\Upsilon,y) = (\vec{\mathbf{z}^{**}} - \vec{\mathbf{r}^{**}})(\Upsilon,y), \ \forall(\Upsilon,y)\in\Lambda_{1,\varepsilon}^{**,1}, \\ \vec{\mathbf{w}^{**}}_l(\Upsilon,y) = \vec{\mathbf{0}}, \ \forall(\Upsilon,y)\in\Lambda_{2,\varepsilon}^{**,1}\cup\Lambda_{3,\varepsilon}^{**,1}\cup\Lambda_{4,\varepsilon}^{**,1}, \end{cases} \tag{2.14}$$

when $\alpha\mu^2 > \lambda\varepsilon$, where $\Omega_\varepsilon^{**,1} = (0,\frac{\mu}{\varepsilon})\times(0,1)$ and $\Lambda_{i,\varepsilon}^{**,1}$, $i=1,2,3,4$ are the corresponding boundaries of the domain $\Omega_\varepsilon^{**,1}$. Then, using the same techniques that in [28,29], we can obtain the bounds (2.11) and (2.12) for the left boundary layer function $\mathbf{w^{**}}_l$. □

Similarly, as has been done for $\vec{\mathbf{w}}_l$, the left edge of Ω, we can consider the corresponding boundary layer components $\vec{\mathbf{w}}_b$, $\vec{\mathbf{w}}_r$, $\vec{\mathbf{w}}_t$ for which we can obtain similar bounds as those in Lemma 2.7.

Finally, related to the corner at $(0,0)$ in Ω, we consider the corner layer component $\vec{\mathbf{s}}_{lb}$, which is the solution of the problem

$$\mathcal{L}_{\varepsilon,\mu}\vec{\mathbf{s}}_{lb}(x,y) = \vec{\mathbf{0}}, \quad \forall(x,y)\in\Omega, \tag{2.15a}$$

$$\vec{\mathbf{s}}_{lb}(x,y) = -\vec{\mathbf{w}}_l(x,y), \ \forall(x,y)\in\Lambda_1, \tag{2.15b}$$

$$\vec{\mathbf{s}}_{lb}(x,y) = -\vec{\mathbf{w}}_b(x,y), \ \forall(x,y)\in\Lambda_2, \tag{2.15c}$$

$$\vec{\mathbf{s}}_{lb}(x,y) = 0, \ \forall(x,y)\in\Lambda_3\cup\Lambda_4. \tag{2.15d}$$

Lemma 2.8. *Let $\vec{\mathbf{s}}_{lb}$ be the corner layer component satisfying the equations in (2.15). If $\alpha\mu^2 \le \lambda\varepsilon$, then it holds*

$$|\vec{\mathbf{s}}_{lb}(x,y)| \le C\exp\left(-\sqrt{\frac{\alpha_1\lambda}{\varepsilon}}x\right)\exp\left(-\sqrt{\frac{\alpha_2\lambda}{\varepsilon}}y\right), \quad \left\|\frac{\partial^{i+j}\vec{\mathbf{s}}_{lb}}{\partial x^i\partial y^j}\right\| \le C(1+\varepsilon^{-(i+j)/2}), \quad 1\le i+j\le 4. \tag{2.16}$$

On the other hand, if $\alpha\mu^2 > \lambda\varepsilon$, then it holds

$$|\vec{\mathbf{s}}_{lb}(x,y)| \le C\exp\left(-\frac{\alpha_1\mu}{\varepsilon}x\right)\exp\left(-\frac{\alpha_2\mu}{\varepsilon}y\right), \quad \left\|\frac{\partial^{i+j}\vec{\mathbf{s}}_{lb}}{\partial x^i\partial y^j}\right\| \le C\left(\frac{\varepsilon}{\mu}\right)^{-(i+j)}, \quad 1\le i+j\le 4, \tag{2.17}$$

where λ is defined in (1.3).

Proof. We consider the stretching variables $\zeta = \frac{x}{\sqrt{\varepsilon}}$, $\xi = \frac{y}{\sqrt{\varepsilon}}$ for $\alpha\mu^2 \le \lambda\varepsilon$ and $\Upsilon = \frac{\mu x}{\varepsilon}$, $\varphi = \frac{\mu y}{\varepsilon}$ for $\alpha\mu^2 > \lambda\varepsilon$ to obtain the bounds for the corner layer component $\vec{\mathbf{s}}_{lb}$; then, the resulting continuous problems after this change of variable, are given by

$$\begin{cases} \left(\frac{\partial^2 \vec{\mathbf{s}^*}_{lb}}{\partial\zeta^2} + \frac{\partial^2 \vec{\mathbf{s}^*}_{lb}}{\partial\xi^2}\right) + \mu\varepsilon^{-1/2}\vec{\mathbf{A}}^*(\zeta,\xi)\frac{\partial \vec{\mathbf{s}^*}_{lb}}{\partial\zeta} + \mu\varepsilon^{-1/2}\vec{\mathbf{B}}^*(\zeta,\xi)\frac{\partial \vec{\mathbf{s}^*}_{lb}}{\partial\xi} - \\ \qquad \vec{\mathbf{C}}^*(\zeta,\xi)\vec{\mathbf{s}^*}_{lb} = \vec{\mathbf{f}}^*(\zeta,\xi),\ \forall(\zeta,\xi) \in \Omega_\varepsilon^{*,2}, \\ \vec{\mathbf{s}^*}_{lb}(\zeta,\xi) = -\vec{\mathbf{w}^*}_l(\zeta,\xi),\ \forall(\zeta,\xi) \in \Lambda_{1,\varepsilon}^{*,2}, \\ \vec{\mathbf{s}^*}_{lb}(\zeta,\xi) = -\vec{\mathbf{w}^*}_b(\zeta,\xi),\ \forall(\zeta,\xi) \in \Lambda_{2,\varepsilon}^{*,2}, \\ \vec{\mathbf{s}^*}_{lb}(\zeta,\xi) = \vec{\mathbf{0}},\ \forall(\zeta,\xi) \in \Lambda_{3,\varepsilon}^{*,2} \cup \Lambda_{4,\varepsilon}^{*,2}, \end{cases} \tag{2.18}$$

in the case that $\alpha\mu^2 \le \lambda\varepsilon$, where $\Omega_\varepsilon^{*,2} = (0, \frac{1}{\sqrt{\varepsilon}})^2$ and $\Lambda_{i,\varepsilon}^{*,2}$, $i = 1,2,3,4$ are the relative boundaries of the domain $\Omega_\varepsilon^{*,2}$, and by

$$\begin{cases} \left(\varepsilon^{-1}\frac{\partial^2 \vec{\mathbf{s}^{**}}_{lb}}{\partial\Upsilon^2} + \varepsilon^{-1}\frac{\partial^2 \vec{\mathbf{s}^{**}}_{lb}}{\partial\varphi^2}\right) + \varepsilon^{-1}\vec{\mathbf{A}}^{**}(\Upsilon,\varphi)\frac{\partial \vec{\mathbf{s}^{**}}_{lb}}{\partial\Upsilon} + \varepsilon^{-1}\vec{\mathbf{B}}^{**}(\Upsilon,\varphi)\frac{\partial \vec{\mathbf{s}^{**}}_{lb}}{\partial\varphi} - \\ \qquad \mu^{-2}\vec{\mathbf{C}}^{**}(\Upsilon,\varphi)\vec{\mathbf{s}^{**}}_{lb} = \mu^{-2}\vec{\mathbf{f}}^{**}(\Upsilon,\varphi),\ \forall(\Upsilon,\varphi) \in \Omega_\varepsilon^{**,2}, \\ \vec{\mathbf{s}^{**}}_{lb}(\Upsilon,\varphi) = -\vec{\mathbf{w}^{**}}_l(\Upsilon,\varphi),\ \forall(\Upsilon,\varphi) \in \Lambda_{1,\varepsilon}^{**,2}, \\ \vec{\mathbf{s}^{**}}_{lb}(\Upsilon,\varphi) = -\vec{\mathbf{w}^{**}}_b(\Upsilon,\varphi),\ \forall(\Upsilon,\varphi) \in \Lambda_{2,\varepsilon}^{**,2}, \\ \vec{\mathbf{s}^{**}}_{lb}(\Upsilon,\varphi) = \vec{\mathbf{0}},\ \forall(\Upsilon,\varphi) \in \Lambda_{3,\varepsilon}^{**,2} \cup \Lambda_{4,\varepsilon}^{**,2}, \end{cases} \tag{2.19}$$

when $\alpha\mu^2 > \lambda\varepsilon$, where $\Omega_\varepsilon^{**,2} = (0, \frac{\mu}{\varepsilon})^2$ and $\Lambda_{i,\varepsilon}^{**,2}$, $i = 1,2,3,4$ are the relative boundaries of the domain $\Omega_\varepsilon^{**,2}$. Then, using the same techniques that in [28,29]. we can get the bounds (2.16) and (2.17) for the corner layer function $\vec{\mathbf{s}}_{lb}$. □

Similarly, we can describe the other corner layer components $\vec{\mathbf{s}}_{br}$, $\vec{\mathbf{s}}_{rt}$ and $\vec{\mathbf{s}}_{lt}$, corresponding to the different corners of Ω, which satisfy similar bounds as those ones in Lemma 2.8.

Following result give bounds on derivatives of the exact solution of problem (1.1) in the continuous maximum norm; this result is required posteriorly for the analysis of the uniform convergence of the numerical method defined below.

Theorem 2.9. *The solution $\vec{\mathbf{z}}$ of (1.1), assuming that (1.2) holds, can be written as*

$$\vec{\mathbf{z}}(x,y) = \vec{\mathbf{r}}(x,y) + \vec{\mathbf{w}}(x,y) + \vec{\mathbf{s}}(x,y),$$

where

$$\mathcal{L}_{\epsilon,\mu}\vec{\mathbf{r}}(x,y) = \vec{\mathbf{f}}(x,y), \quad \mathcal{L}_{\varepsilon,\mu}\vec{\mathbf{w}}(x,y) = \vec{\mathbf{0}}, \quad \mathcal{L}_{\varepsilon,\mu}\vec{\mathbf{s}}(x,y) = \vec{\mathbf{0}},$$

and

$$\begin{aligned} \vec{\mathbf{w}}(x,y) &= \vec{\mathbf{w}}_l(x,y) + \vec{\mathbf{w}}_r(x,y) + \vec{\mathbf{w}}_b(x,y) + \vec{\mathbf{w}}_t(x,y), \\ \vec{\mathbf{s}}(x,y) &= \vec{\mathbf{s}}_{lb}(x,y) + \vec{\mathbf{s}}_{br}(x,y) + \vec{\mathbf{s}}_{rt}(x,y) + \vec{\mathbf{s}}_{lt}(x,y). \end{aligned}$$

Furthermore, the regular and singular components and their derivatives satisfy the following bounds

$$\begin{cases} \left\| \frac{\partial^{i+j}\vec{\mathbf{r}}}{\partial x^i \partial y^j} \right\| \le C(1 + \varepsilon^{1-(i+j)/2}), \quad 1 \le i+j \le 4,\ \text{if } \alpha\mu^2 \le \lambda\varepsilon, \\ \left\| \frac{\partial^{i+j}\vec{\mathbf{r}}}{\partial x^i \partial y^j} \right\| \le C(1 + (\frac{\varepsilon}{\mu})^{2-(i+j)}), \quad 1 \le i+j \le 4,\ \text{if } \alpha\mu^2 > \lambda\varepsilon, \end{cases}$$

$$\begin{cases} |\vec{\mathbf{w}}_l(x,y)| \le Ce^{-\alpha_1\theta_1 x}; \\ |\vec{\mathbf{w}}_b(x,y)| \le Ce^{-\alpha_2\theta_1 y}; \\ |\vec{\mathbf{w}}_r(x,y)| \le Ce^{-\alpha_1\theta_2(1-x)}; \\ |\vec{\mathbf{w}}_t(x,y)| \le Ce^{-\alpha_2\theta_2(1-y)}; \end{cases} \qquad \begin{cases} |\vec{\mathbf{s}}_{lb}(x,y)| \le Ce^{-\alpha_1\theta_1 x}e^{-\alpha_2\theta_1 y}, \\ |\vec{\mathbf{s}}_{br}(x,y)| \le Ce^{-\alpha_1\theta_2(1-x)}e^{-\alpha_2\theta_1 y}, \\ |\vec{\mathbf{s}}_{rt}(x,y)| \le Ce^{-\alpha_1\theta_2(1-x)}e^{-\alpha_2\theta_2(1-y)}, \\ |\vec{\mathbf{s}}_{lt}(x,y)| \le Ce^{-\alpha_1\theta_1 x}e^{-\alpha_2\theta_2(1-y)}, \end{cases}$$

$$\text{where } \theta_1 = \begin{cases} \sqrt{\frac{\lambda}{\varepsilon}},\ \alpha\mu^2 \le \lambda\varepsilon, \\ \frac{\mu}{\varepsilon},\ \mu^2 > \lambda\epsilon, \end{cases} \quad \theta_2 = \begin{cases} \sqrt{\frac{\lambda}{2\varepsilon}},\ \alpha\mu^2 \le \lambda\varepsilon, \\ \frac{\lambda}{2\mu},\ \alpha\mu^2 > \lambda\varepsilon, \end{cases} \tag{2.20}$$

$$\begin{cases} \left\{ \left\| \dfrac{\partial^i \vec{\mathbf{w}}_b}{\partial x^i} \right\|, \left\| \dfrac{\partial^i \vec{\mathbf{w}}_t}{\partial x^i} \right\| \right\} \le C(1+\varepsilon^{(1-i)/2}), & \textit{where } 1 \le i \le 4, \ \textit{if } \alpha\mu^2 \le \lambda\varepsilon, \\ \left\| \dfrac{\partial^i \vec{\mathbf{w}}_b}{\partial x^i} \right\| \le C\left(1+\left(\dfrac{\varepsilon}{\mu}\right)^{1-i}\right), & \textit{where } 1 \le i \le 4, \ \textit{if } \alpha\mu^2 > \lambda\varepsilon, \\ \left\| \dfrac{\partial^i \vec{\mathbf{w}}_t}{\partial x^i} \right\| \le C\left(1+\left(\dfrac{1}{\mu}\right)^{i-1}\right), & \textit{where } 1 \le i \le 4, \ \textit{if } \alpha\mu^2 > \lambda\varepsilon, \end{cases}$$

$$\begin{cases} \left\{ \left\| \dfrac{\partial^j \vec{\mathbf{w}}_l}{\partial y^j} \right\|, \left\| \dfrac{\partial^j \vec{\mathbf{w}}_r}{\partial y^j} \right\| \right\} \le C(1+\varepsilon^{(1-j)/2}), & \textit{where } 1 \le j \le 4, \ \textit{if } \alpha\mu^2 \le \lambda\varepsilon, \\ \left\| \dfrac{\partial^j \vec{\mathbf{w}}_l}{\partial y^j} \right\| \le C\left(1+\left(\dfrac{\varepsilon}{\mu}\right)^{1-j}\right), & \textit{where } 1 \le j \le 4, \ \textit{if } \alpha\mu^2 > \lambda\varepsilon, \\ \left\| \dfrac{\partial^j \vec{\mathbf{w}}_r}{\partial y^j} \right\| \le C\left(1+\left(\dfrac{1}{\mu}\right)^{j-1}\right), & \textit{where } 1 \le j \le 4, \ \textit{if } \alpha\mu^2 > \lambda\varepsilon, \end{cases}$$

$$\begin{cases} \max\left\{ \left\| \dfrac{\partial^{i+j} \vec{\mathbf{s}}_{lb}}{\partial x^i \partial y^j} \right\|, \left\| \dfrac{\partial^{i+j} \vec{\mathbf{s}}_{br}}{\partial x^i \partial y^j} \right\|, \left\| \dfrac{\partial^{i+j} \vec{\mathbf{s}}_{rt}}{\partial x^i \partial y^j} \right\|, \left\| \dfrac{\partial^{i+j} \vec{\mathbf{s}}_{lt}}{\partial x^i \partial y^j} \right\| \right\} \le C\varepsilon^{-(i+j)/2}, & \textit{where } 1 \le i+j \le 4, \ \textit{if } \alpha\mu^2 \le \lambda\varepsilon, \\ \left\| \dfrac{\partial^{i+j} \vec{\mathbf{s}}_{lb}}{\partial x^i \partial y^j} \right\| \le C\left(\dfrac{\varepsilon}{\mu}\right)^{-(i+j)}, & \textit{where } 1 \le i+j \le 4, \ \textit{if } \alpha\mu^2 > \lambda\varepsilon, \\ \left\| \dfrac{\partial^{i+j} \vec{\mathbf{s}}_{br}}{\partial x^i \partial y^j} \right\| \le C\left(\dfrac{1}{\mu}\right)^{i}\left(\dfrac{\varepsilon}{\mu}\right)^{-j}, & \textit{where } 1 \le i+j \le 4, \ \textit{if } \alpha\mu^2 > \lambda\varepsilon, \\ \left\| \dfrac{\partial^{i+j} \vec{\mathbf{s}}_{rt}}{\partial x^i \partial y^j} \right\| \le C\left(\dfrac{\varepsilon}{\mu}\right)^{-i}\left(\dfrac{1}{\mu}\right)^{j}, & \textit{where } 1 \le i+j \le 4, \ \textit{if } \alpha\mu^2 > \lambda\varepsilon, \\ \left\| \dfrac{\partial^{i+j} \vec{\mathbf{s}}_{lt}}{\partial x^i \partial y^j} \right\| \le C\left(\dfrac{1}{\mu}\right)^{i+j}, & \textit{where } 1 \le i \le 4, \ \textit{if } \alpha\mu^2 > \lambda\varepsilon. \end{cases}$$

Proof. The proof follows directly from Lemmas 2.4, 2.7 and 2.8. □

3. Discretization of the problem

3.1. Bakhvalov–Shishkin mesh

In this section, we construct the B-S-mesh for the problem (1.1) and we define the finite difference scheme on the domain $\Omega^{N,N} = \{(x_i, y_j) : 0 \le i, j \le N\}$. To make an appropriate fitted nonuniform mesh, we first subdivided the unit interval in x- and y-directions into three subintervals each as

$$[0, 1] = [0, \sigma_1] \cup [\sigma_1, 1-\sigma_2] \cup [1-\sigma_2, 1],$$

where the transition point σ_1 and σ_2 are given by

$$\sigma_1 = \min\left\{\frac{1}{4}, \frac{2}{\theta_1}\ln N\right\}, \ \sigma_2 = \min\left\{\frac{1}{4}, \frac{2}{\theta_2}\ln N\right\}, \tag{3.1}$$

where θ_1 and θ_2 are defined in (2.20).

For simplicity, we take the same number of mesh points for both spatial variables. On each subinterval in x and y-axis, $[\sigma_1, 1-\sigma_2]$ are $N/2$ length, while the rest subintervals $[0, \sigma_1]$, $[1-\sigma_2, 1]$ are divided by using the mesh generating functions $\Phi_i(t)$, $i = 1, 2$, where Φ_1 and Φ_2 are monotonically increasing and decreasing, respectively, which satisfy

$$\Phi_1(0) = 0, \ \Phi_1(1/4) = \ln N, \ \Phi_2(3/4) = \ln N, \ \Phi_2(1) = 0.$$

As it is usual, in the context of this type of meshes, now we define two new functions Ψ_i, $i = 1, 2$, that are closely related to Φ_i, $i = 1, 2$, by $\Phi_1 = -\ln \Psi_1$, and $\Phi_2 = -\ln \Psi_2$.

In the literature, there are numerous mesh characterizing functions, but we will only use those that correlate to B-S-mesh [30], which is defined in the following way.

- Bakhvalov–Shishkin mesh (**B-S**-mesh). The function Ψ_1 is given by

$$\Psi_1(t) = 1 - 4(1-N^{-1})t, \ \Psi_2(t) = 1 - 4(1-N^{-1})(1-t).$$

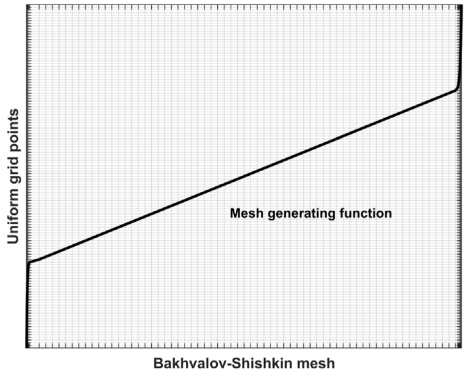

(a) B-S mesh for $\mu = 1.e-7, \varepsilon = 1.e-6$

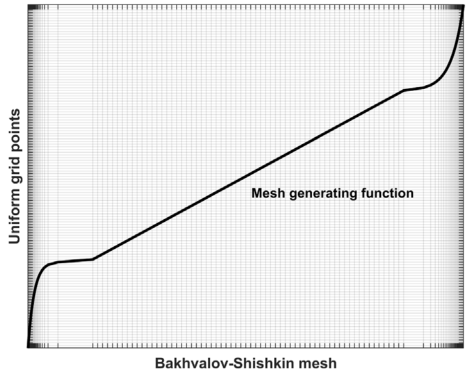

(b) B-S mesh for $\mu = 1.e-7, \varepsilon = 1.e-4$

Fig. 1. Bakhvalov-Shishkin meshes.

The grid points of the x-space variable are defined by

$$x_i = \begin{cases} \frac{2}{\theta_1}\Phi_1(t_i), & \text{if} \quad 0 \le i \le N/4-1, \\ \sigma_1 + \frac{2}{N}(1-\sigma_1-\sigma_2)(i-\frac{N}{4}), & \text{if} \quad N/4 \le i \le 3N/4, \\ 1 - 2\frac{2}{\theta_2}\Phi_2(t_i), & \text{if} \quad 3N/4+1 \le i \le N, \end{cases}$$

where $t_i = \dfrac{i}{N}$, $i = 0, 1, \ldots, N$. The step sizes are given by $h_i = x_i - x_{i-1}$, $i = 1, 2, \ldots, N$, $\bar{h}_i = h_i + h_{i+1}$, $i = 1, 2, \ldots, N-1$.

To see the type of mesh that we obtain, Fig. 1 displays the mesh for two different cases.

Using the preceding definition, on the coarse mesh we have

$$h_i = H_1 = \frac{2}{N}(1-\sigma_1-\sigma_2), \text{ for} \quad N/4 \le i \le 3N/4. \tag{3.2}$$

and on the fine mesh it holds

$$\begin{cases} h_i \ge h_{i+1}, & \text{for} \quad 0 \le i \le N/4+1, \\ h_i \le h_{i+1}, & \text{for} \quad 3N/4+1 \le i \le N. \end{cases}$$

Similarly, we can define the mesh points and the mesh-generating functions for $y_j,\ j = 0, 1, \ldots, N$. The boundaries of the domain $\Omega^{N,N}$ are denoted as

$$\Lambda_1^{N,N} = \left\{(0, y_j) \,\middle|\, 0 \le j \le N\right\}, \Lambda_2^{N,N} = \left\{(x_i, 0) \,\middle|\, 0 \le i \le N\right\},$$
$$\Lambda_3^{N,N} = \left\{(1, y_j) \,\middle|\, 0 \le j \le N\right\}, \Lambda_4^{N,N} = \left\{(x_i, 1) \,\middle|\, 0 \le i \le N\right\},$$

and $\Lambda^{N,N} = \Lambda_1^{N,N} \cup \Lambda_2^{N,N} \cup \Lambda_3^{N,N} \cup \Lambda_4^{N,N}$.

Remark 3.1. Note that the mesh-generating functions in x-space, $\Phi_i,\ i = 1, 2$, satisfy the following conditions

$$\max_{t\in[0,1/4]} |\Phi_1'(t)| \le CN, \quad \max_{t\in[3/4,1]} |\Phi_2'(t)| \le CN, \tag{3.3}$$

and

$$\int_0^{1/4} \{\Phi_1'(t)\}^2 dt \le CN, \quad \int_{3/4}^1 \{\Phi_2'(t)\}^2 dt \le CN. \tag{3.4}$$

Using the above assumptions and a similar argument to this one given in [31], we can prove that $h_i \le CN^{-1}$ for $1 \le i \le N$. Analogous estimates hold true for the $y-$variable.

3.2. Finite difference method (FDM)

On an arbitrary mesh, $\bar{\Omega}^{N,N}$, in order to discretize the problem (1.1), we define the standard upwind finite difference operator, given by

$$\begin{cases} \mathcal{L}^{N,N}_{\varepsilon,\mu}\vec{\mathbf{Z}}(x_i,y_j) = \vec{\mathbf{f}}(x_i,y_j), \ \forall (x_i,y_j) \in \Omega^{N,N}, \\ \vec{\mathbf{Z}}(x_i,y_j) = \vec{\mathbf{g}}_1(y_j), \ (x_i,y_j) \in \Lambda^{N,N}_1, \quad \vec{\mathbf{Z}}(x_i,y_j) = \vec{\mathbf{g}}_2(x_i), \ (x_i,y_j) \in \Lambda^{N,N}_2, \\ \vec{\mathbf{Z}}(x_i,y_j) = \vec{\mathbf{g}}_3(y_j), \ (x_i,y_j) \in \Lambda^{N,N}_3, \quad \vec{\mathbf{Z}}(x_i,y_j) = \vec{\mathbf{g}}_4(x_i), \ (x_i,y_j) \in \Lambda^{N,N}_4, \end{cases} \tag{3.5}$$

where

$$\mathcal{L}^{N,N}_{\varepsilon,\mu}\vec{\mathbf{Z}}(x_i,y_j) = \varepsilon(\delta^2_{xx}+\delta^2_{yy})\vec{\mathbf{Z}}(x_i,y_j) + \mu(\vec{\mathbf{A}}(x_i,y_j)D^+_x + \vec{\mathbf{B}}(x_i,y_j)D^+_y)\vec{\mathbf{Z}}(x_i,y_j) - \vec{\mathbf{C}}(x_i,y_j)\vec{\mathbf{Z}}(x_i,y_j).$$

As it is usual, the discrete differential operators D^+_x, D^+_y, δ^2_{xx}, and δ^2_{yy} are given by

$$D^+_x\vec{\mathbf{Z}}(x_i,y_j) = \frac{\vec{\mathbf{Z}}(x_{i+1},y_j)-\vec{\mathbf{Z}}(x_i,y_j)}{h_{i+1}},\ D^-_x\vec{\mathbf{Z}}(x_i,y_j) = \frac{\vec{\mathbf{Z}}(x_i,y_j)-\vec{\mathbf{Z}}(x_{i-1},y_j)}{h_i},$$
$$D^+_y\vec{\mathbf{Z}}(x_i,y_j) = \frac{\vec{\mathbf{Z}}(x_i,y_{j+1})-\vec{\mathbf{Z}}(x_i,y_j)}{k_{j+1}},\ D^-_y\vec{\mathbf{Z}}(x_i,y_j) = \frac{\vec{\mathbf{Z}}(x_i,y_j)-\vec{\mathbf{Z}}(x_i,y_{j-1})}{k_j},$$
$$\delta^2_{xx}\vec{\mathbf{Z}}(x_i,y_j) = \frac{2}{\bar{h}_i}(D^+_x\vec{\mathbf{Z}}(x_i,y_j)-D^-_x\vec{\mathbf{Z}}(x_i,y_j)),\ \delta^2_{yy}\vec{\mathbf{Z}}(x_i,y_j) = \frac{2}{\bar{k}_j}(D^+_y\vec{\mathbf{Z}}(x_i,y_j)-D^-_y\vec{\mathbf{Z}}(x_i,y_j)),$$

for $i,j = 1,2,\ldots,N-1$.

Lemma 3.2 (*Discrete Minimum Principle*)**.** *Let $\mathcal{L}^{N,N}_{\varepsilon,\mu}$ be the discrete operator given in (3.5), If $\vec{\mathbf{\Phi}}(x_i,y_j) \geq \vec{\mathbf{0}}$ on $\Lambda^{N,N}$, and $\mathcal{L}^{N,N}_{\varepsilon,\mu}\vec{\mathbf{\Phi}}(x_i,y_j) \leq \vec{\mathbf{0}}$, $\forall (x_i,y_j) \in \Omega^{N,N}$, then $\vec{\boldsymbol{\phi}}(x_i,y_j) \geq \vec{\mathbf{0}}$, $\forall (x_i,y_j) \in \bar{\Omega}^{N,N}$.*

Proof. We can prove this Lemma following the ideas in [29,32]. □

Lemma 3.3 (*Discrete Stability Result*)**.** *Let $\vec{\mathbf{Z}}(x_i,y_j)$ be the solution of (3.5). Then it holds*

$$\|\vec{\mathbf{Z}}(x_i,y_j)\|_{\bar{\Omega}^{N,N}} \leq \frac{1}{\alpha}\|\mathcal{L}^{N,N}_{\varepsilon,\mu}\vec{\mathbf{Z}}\|_{\Omega^{N,N}} + \max\left\{\|\vec{\mathbf{Z}}\|_{\Lambda^{N,N}_1}, \|\vec{\mathbf{Z}}\|_{\Lambda^{N,N}_2}, \|\vec{\mathbf{Z}}\|_{\Lambda^{N,N}_3}, \|\vec{\mathbf{Z}}\|_{\Lambda^{N,N}_4}\right\},$$

where $\|.\|_{\bar{\Omega}^{N,N}}$ denotes the discrete pointwise maximum norm on $\bar{\Omega}^{N,N}$.

Proof. We consider the barrier function

$$\vec{\mathbf{\Phi}}^{\pm}(x_i,y_j) = \frac{1}{\alpha}\|\mathcal{L}^{N,N}_{\varepsilon,\mu}\vec{\mathbf{z}}\|_{\bar{\Omega}^{N,N}} + \max\left\{\|\vec{\mathbf{z}}\|_{\Lambda^{N,N}_1}, \|\vec{\mathbf{z}}\|_{\Lambda^{N,N}_2}, \|\vec{\mathbf{z}}\|_{\Lambda^{N,N}_3}, \|\vec{\mathbf{z}}\|_{\Lambda^{N,N}_4}\right\} \pm \vec{\mathbf{z}}(x_i,y_j),$$

and it can be proved easily using Lemma 3.2. □

4. Uniform convergence of the numerical method

In this section we prove the uniform convergence of the numerical method (3.5) when it is constructed on the B-S mesh. As like for the continuous solution, we decompose the discrete solution into smooth component, boundary and corner layer components, to estimate the nodal error independently, such as

$$\vec{\mathbf{Z}}(x_i,y_j) = \vec{\mathbf{R}}(x_i,y_j) + \vec{\mathbf{W}}(x_i,y_j) + \vec{\mathbf{S}}(x_i,y_j),$$

where

$$\vec{\mathbf{W}}(x_i,y_j) = \vec{\mathbf{W}}_l(x_i,y_j) + \vec{\mathbf{W}}_r(x_i,y_j) + \vec{\mathbf{W}}_b(x_i,y_j) + \vec{\mathbf{W}}_t(x_i,y_j),$$
$$\vec{\mathbf{S}}(x_i,y_j) = \vec{\mathbf{S}}_{lb}(x_i,y_j) + \vec{\mathbf{S}}_{br}(x_i,y_j) + \vec{\mathbf{S}}_{rt}(x_i,y_j) + \vec{\mathbf{S}}_{lt}(x_i,y_j).$$

First, the smooth component $\vec{\mathbf{R}}(x,y)$ is the solution of the problem

$$\begin{cases} \mathcal{L}^{N,N}_{\varepsilon,\mu}\vec{\mathbf{R}}(x_i,y_j) = \vec{\mathbf{F}}(x,y), \quad \forall (x_i,y_j) \in \Omega^{N,N}, \\ \vec{\mathbf{R}}(x_i,y_j) = \vec{\mathbf{r}}(x_i,y_j), \quad \forall (x_i,y_j) \in \Lambda^{N,N}. \end{cases} \tag{4.1}$$

Hence, the boundary and corner layer components $\vec{\mathbf{W}}(x,y)$ and $\vec{\mathbf{S}}(x,y)$, are defined as the solutions of the problems

$$\begin{cases} \mathcal{L}^{N,N}_{\varepsilon,\mu}\vec{\mathbf{W}}(x_i,y_j) = \vec{\mathbf{0}}, \quad \forall (x_i,y_j) \in \Omega^{N,N}, \\ \vec{\mathbf{W}}(x_i,y_j) = \vec{\mathbf{w}}(x_i,y_j), \quad \forall (x_i,y_j) \in \Lambda^{N,N}, \end{cases} \tag{4.2}$$

and

$$\begin{cases} \mathcal{L}^{N,N}_{\varepsilon,\mu}\vec{\mathbf{S}}(x_i,y_j)=\vec{\mathbf{0}}, & \forall(x_i,y_j)\in\Omega^{N,N},\\ \vec{\mathbf{S}}(x_i,y_j)=\vec{\mathbf{s}}(x_i,y_j), & \forall(x_i,y_j)\in\Lambda^{N,N}, \end{cases} \tag{4.3}$$

respectively.

Lemma 4.1. *Consider $\vec{\mathbf{r}}$ and $\vec{\mathbf{R}}$ are the continuous and the discrete solutions of* (2.3) and (4.1)*, respectively. Then, for both the cases $\alpha\mu^2\le\lambda\varepsilon$ and $\alpha\mu^2>\lambda\varepsilon$ we have*

$$|\vec{\mathbf{R}}(x_i,y_j)-\vec{\mathbf{r}}(x_i,y_j)|\le CN^{-1},$$

where λ is defined in (1.3).

Proof. The truncation error for the regular components (4.1) gives the following estimates based on the results in Lemma 2.4:

$$|\mathcal{L}^{N,N}_{\varepsilon,\mu}(\vec{\mathbf{R}}(x_i,y_j)-\vec{\mathbf{r}}(x_i,y_j))|\le C\left[(h_i+h_{i+1})\left(\varepsilon\left\|\frac{\partial^3\vec{\mathbf{r}}}{\partial x^3}\right\|+\mu\left\|\frac{\partial^2\vec{\mathbf{r}}}{\partial x^2}\right\|\right)+(k_j+k_{j+1})\left(\varepsilon\left\|\frac{\partial^3\vec{\mathbf{r}}}{\partial y^3}\right\|+\mu\left\|\frac{\partial^2\vec{\mathbf{r}}}{\partial y^2}\right\|\right)\right]. \tag{4.4}$$

Therefore, it follows

$$|\mathcal{L}^{N,N}_{\varepsilon,\mu}(\vec{\mathbf{R}}(x_i,y_j)-\vec{\mathbf{r}}(x_i,y_j))|\le\begin{cases} C(N^{-1}\sqrt{\varepsilon}), & \text{if } \alpha\mu^2\le\lambda\varepsilon,\\ C(N^{-1}\mu), & \text{if } \alpha\mu^2>\lambda\varepsilon. \end{cases} \tag{4.5}$$

Using a suitable barrier function and Lemma 3.2, we can obtain

$$\|\vec{\mathbf{R}}(x_i,y_j)-\vec{\mathbf{r}}(x_i,y_j)\|\le CN^{-1},\ \ \forall(x_i,y_j)\in\Omega^{N,N}, \tag{4.6}$$

which is the required result. □

Applying the arguments of ([29], Theorem 8.1), we show the ϵ-uniform bounds of the corner and edge components errors using evidence-based on suitable barrier functions. The following barrier functions are considered:

$$\begin{cases} \mathfrak{B}_{\vec{\mathbf{w}}_l;i}=\begin{cases}\prod_{\iota=1}^{i}(1+h_\iota\theta_1)^{-1}, & i\ne 0,\\ 1, & i=0,\end{cases} & \mathfrak{B}_{\vec{\mathbf{w}}_r;i}=\begin{cases}\prod_{\iota=i+1}^{N}(1+h_\iota\theta_2)^{-1}, & i\ne N,\\ 1, & i=N,\end{cases}\\ \mathfrak{B}_{\vec{\mathbf{w}}_b;j}=\begin{cases}\prod_{\iota=1}^{j}(1+k_\iota\theta_1)^{-1}, & j\ne 0,\\ 1, & j=0,\end{cases} & \mathfrak{B}_{\vec{\mathbf{w}}_t;j}=\begin{cases}\prod_{\iota=1}^{j}(1+k_\iota\theta_2)^{-1}, & j\ne N,\\ 1, & j=N,\end{cases} \end{cases}$$

and for all i, it holds

$$\exp(-\theta_1x_i)=\prod_{\iota=1}^{i}\exp(-\theta_1h_\iota)\le\mathfrak{B}_{\vec{\mathbf{w}}_{l,i}}, \tag{4.7}$$

and for $N/4\le i\le N$, we have

$$\mathfrak{B}_{\vec{\mathbf{w}}_{l,i}}\le\mathfrak{B}_{\vec{\mathbf{w}}_{l,N/4}}=\left(1+\frac{8\ln N}{N}\right)^{-N/4}\le CN^{-1}. \tag{4.8}$$

For the remaining boundary layer functions, equivalent bounds can be obtained.

Lemma 4.2. *If $\vec{\mathbf{w}}_l$ and $\vec{\mathbf{W}}_l$ are the continuous and the discrete solutions of* (2.10) and (4.2)*, respectively, then it holds*

$$|\vec{\mathbf{w}}_l(x_i,y_j)-\vec{\mathbf{W}}_l(x_i,y_j)|\le\begin{cases} CN^{-1}, & \textit{if}\ \ \alpha\mu^2\le\lambda\varepsilon,\\ CN^{-1}, & \textit{if}\ \ \alpha\mu^2>\lambda\varepsilon, \end{cases}$$

where λ is defined in (1.3).

Proof. If $\sigma_1=1/4$, the proof can be obtained using standard techniques by taking into account that $\varepsilon^{-1}\le C\ln^2N$ when $\alpha\mu^2\le\lambda\varepsilon$ and $(\frac{\varepsilon}{\mu})^{-1}\le C\ln N$ when $\alpha\mu^2>\lambda\varepsilon$.

Thus, we will assume that $\sigma_1=1/4$, which is the most interesting case. Here we merely provide the details corresponding to the edge layer function $\vec{\mathbf{w}}_l$. Similar results hold for the remaining boundary layer components. From (4.2) and Theorem 2.9, we have

$$|\vec{\mathbf{W}}_l(x_i,y_j)|=|\vec{\mathbf{w}}_l(x_i,y_j)|\le Ce^{-\theta_1x_i}\le C\mathfrak{B}_{\vec{\mathbf{w}}_{l,i}},\quad\forall(x_i,y_j)\in\Lambda^{N,N}. \tag{4.9}$$

Further, for all grid points $(x_i, y_j) \in \Omega^{N,N}$, from (4.2), (4.7), and the discrete minimum principle, we have

$$|\vec{\mathbf{W}}_l(x_i, y_j)| \le \mathfrak{B}_{\vec{\mathbf{w}}_{l,i}}. \tag{4.10}$$

After applying (4.10) and Theorem 2.9, we conclude that

$$|\vec{\mathbf{w}}_l(x_i, y_j) - \vec{\mathbf{W}}_l(x_i, y_j)| \le |\vec{\mathbf{w}}_l(x_i, y_j)| + |\vec{\mathbf{W}}_l(x_i, y_j)| \le C\mathfrak{B}_{\vec{\mathbf{w}}_{l,i}}.$$

Finally, from (4.8), we have

$$|\vec{\mathbf{w}}_l(x_i, y_j) - \vec{\mathbf{W}}_l(x_i, y_j)| \le CN^{-1}, \qquad N/4 \le i \le N,\ 0 \le j \le N. \tag{4.11}$$

To get appropriate bounds of the error in the region $\Omega_1^{N,N} = \{(x_i, y_j) \mid 0 < i < N/4,\ 0 < j < N\}$, we proceed as follows. Applying Taylor expansions, we get

$$|\mathcal{L}^{N,N}_{\varepsilon,\mu}[\vec{\mathbf{W}}_l - \vec{\mathbf{w}}_l](x_i, y_j)| \le C\varepsilon\left(\bar{h}_i\left\|\frac{\partial^3\vec{\mathbf{w}}_l}{\partial x^3}\right\| + \bar{k}_j\left\|\frac{\partial^3\vec{\mathbf{w}}_l}{\partial y^3}\right\|\right) + C\mu\left(h_{i+1}\left\|\frac{\partial^2\vec{\mathbf{w}}_l}{\partial x^2}\right\| + k_{j+1}\left\|\frac{\partial^2\vec{\mathbf{w}}_l}{\partial y^2}\right\|\right). \tag{4.12}$$

If $\alpha\mu^2 \le \lambda\varepsilon$, then, from Theorem 2.9, we have

$$|\mathcal{L}^{N,N}_{\varepsilon,\mu}[\vec{\mathbf{W}}_l(x_i, y_j) - \vec{\mathbf{w}}_l(x_i, y_j)]| \le C(N^{-1}\varepsilon^{-1/2} + \mu(N^{-1}\varepsilon^{-1}) + N^{-1}) \le C\left(\frac{N^{-1}}{\sqrt{\varepsilon}} + N^{-1}\right).$$

Taking the suitable barrier function for the edge layer component $\vec{\mathbf{w}}_l$ as

$$\vec{\Psi}^{\pm}(x_i, y_j) = C\left(\frac{N^{-1}}{\sqrt{\varepsilon}\ln N}(\sigma_1 - x_i) + N^{-1}\right) \pm (\vec{\mathbf{W}}_l(x_i, y_j) - \vec{\mathbf{w}}_l(x_i, y_j)),$$

and using the discrete minimum principle and the above barrier function on $\bar{\Omega}_1^{N,N}$, we can obtain

$$|\vec{\mathbf{w}}_l(x_i, y_j) - \vec{\mathbf{W}}_l(x_i, y_j)| \le CN^{-1}, \quad (x_i, y_j) \in \bar{\Omega}_1^{N,N}. \tag{4.13}$$

Then, the required result follows easily from (4.11) and (4.13).

If $\alpha\mu^2 > \lambda\varepsilon$, then, from Theorem 2.9, we have

$$|\mathcal{L}^{N,N}_{\varepsilon,\mu}[\vec{\mathbf{W}}_l(x_i, y_j) - \vec{\mathbf{w}}_l(x_i, y_j)]| \le C\left(N^{-1}\frac{\mu^2}{\varepsilon} + N^{-1}\right).$$

Taking the suitable barrier function for the boundary layer component $\vec{\mathbf{w}}_l$ as

$$\vec{\Psi}^{\pm}(x_i, y_j) = C\left(\frac{N^{-1}\mu}{\varepsilon\ln N}(\sigma_1 - x_i) + N^{-1}\right) \pm (\vec{\mathbf{W}}_l(x_i, y_j) - \vec{\mathbf{w}}_l(x_i, y_j)),$$

and using the discrete minimum principle and the above barrier function on $\bar{\Omega}_1^{N,N}$, we obtain

$$|\vec{\mathbf{w}}_l(x_i, y_j) - \vec{\mathbf{W}}_l(x_i, y_j)| \le CN^{-1}, \quad (x_i, y_j) \in \bar{\Omega}_1^{N,N}. \tag{4.14}$$

Then, the required result easily follows from (4.11) and (4.14). □

Analogous results hold for the remaining edge layer components $\vec{\mathbf{w}}_b$, $\vec{\mathbf{w}}_r$ and $\vec{\mathbf{w}}_t$, which can be seen in the following lemma.

Lemma 4.3. *At each grid point $(x_i, y_j) \in \Omega^{N,N}$, the error estimate of the bottom, right and top edge layer components for both the cases $\alpha\mu^2 \le \lambda\varepsilon$ and $\alpha\mu^2 > \lambda\varepsilon$ are as follows:*

$$|\vec{\mathbf{w}}_b(x_i, y_j) - \vec{\mathbf{W}}_b(x_i, y_j)| \le CN^{-1},$$
$$|\vec{\mathbf{w}}_r(x_i, y_j) - \vec{\mathbf{W}}_r(x_i, y_j)| \le CN^{-1},$$
$$|\vec{\mathbf{w}}_t(x_i, y_j) - \vec{\mathbf{W}}_t(x_i, y_j)| \le CN^{-1},$$

where λ is defined in (1.3).

Lemma 4.4. *If $\vec{\mathbf{s}}_{lb}$ and $\vec{\mathbf{S}}_{lb}$ are the continuous and discrete solutions of* (2.15) and (4.3), *respectively, then*

$$|\vec{\mathbf{s}}_{lb}(x_i, y_j) - \vec{\mathbf{S}}_{lb}(x_i, y_j)| \le \begin{cases} CN^{-1}, & \text{if} \quad \alpha\mu^2 \le \lambda\epsilon, \\ CN^{-1}, & \text{if} \quad \alpha\mu^2 > \lambda\epsilon, \end{cases} \tag{4.15}$$

where λ is defined in (1.3).

Proof. We only provide the error estimate proof of (4.15) for the corner layer component $\vec{\mathbf{s}}_{lb}$, in the case $\sigma_1 < 1/4$, which is the most interesting case. Proceeding similarly as in Lemma 4.2, we obtain

$$|\vec{\mathbf{S}}_{lb}(x_i, y_j)| \le C \min\{\mathfrak{B}_{\vec{\mathbf{w}}_l}, \mathfrak{B}_{\vec{\mathbf{w}}_b}\}, \quad \text{if } (x_i, y_j) \in \Lambda^{N,N},$$

and also

$$|\vec{\mathbf{s}}_{lb}(x_i, y_j) - \vec{\mathbf{S}}_{lb}(x_i, y_j)| \le C \min\{\mathfrak{B}_{\vec{\mathbf{w}}_l}, \mathfrak{B}_{\vec{\mathbf{w}}_b}\}, \text{ if } (x_i, y_j) \in \Lambda^{N,N}.$$

Then, from (4.8) we can conclude that

$$|\vec{\mathbf{s}}_{lb}(x_i, y_j) - \vec{\mathbf{S}}_{lb}(x_i, y_j)| \le CN^{-1}, \qquad (x_i, y_j) \in \Omega^{N,N} \backslash \Omega^{N,N}_{1,2}, \tag{4.16}$$

where, $\Omega^{N,N}_{1,2} = \{(x_i, y_j) \mid 0 < i, j < N/4\}$. Ultimately, in $\Omega^{N,N}_{1,2}$ the truncation error holds

$$|\mathcal{L}^{N,N}_{\varepsilon,\mu}[\vec{\mathbf{S}}_{lb}(x_i, y_j) - \vec{\mathbf{s}}_{lb}(x_i, y_j)]| \le C\varepsilon\left(\bar{h}_i \left\| \frac{\partial^3 \vec{\mathbf{s}}_{lb}}{\partial x^3} \right\| + \bar{k}_j \left\| \frac{\partial^3 \vec{\mathbf{s}}_{lb}}{\partial y^3} \right\|\right) + C\mu\left(h_i \left\| \frac{\partial^2 \vec{\mathbf{s}}_{lb}}{\partial x^2} \right\| + k_j \left\| \frac{\partial^2 \vec{\mathbf{s}}_{lb}}{\partial y^2} \right\|\right).$$

If $\alpha\mu^2 \le \lambda\varepsilon$, from Theorem 2.9 it follows that

$$|\mathcal{L}^{N,N}_{\varepsilon,\mu}[\vec{\mathbf{S}}_{lb}(x_i, y_j) - \vec{\mathbf{s}}_{lb}(x_i, y_j)]| \le C\frac{\bar{h}_i + \bar{k}_j}{\sqrt{\varepsilon}} \le C\frac{N^{-1}}{\sqrt{\varepsilon}},$$

and using the suitable barrier function

$$\vec{\Psi}^{\pm}(x_i, y_j) = C\left(\frac{N^{-1}}{\sqrt{\varepsilon}\ln N}(\sigma_1 - x_i) + \frac{N^{-1}}{\sqrt{\varepsilon}\ln N}(\sigma_2 - y_j)\right) \pm (\vec{\mathbf{S}}_{lb}(x_i, y_j) - \vec{\mathbf{s}}_{lb}(x_i, y_j))$$

and applying Lemma 3.2 on $\bar{\Omega}^{N,N}_{1,2}$ we obtain

$$|\vec{\mathbf{s}}_{lb}(x_i, y_j) - \vec{\mathbf{S}}_{lb}(x_i, y_j)| \le CN^{-1}, \quad (x_i, y_j) \in \bar{\Omega}^{N,N}_{1,2}. \tag{4.17}$$

Then, the result follows from (4.16) and (4.17). If $\alpha\mu^2 > \lambda\varepsilon$, from Theorem 2.9, we have

$$|\mathcal{L}^{N,N}_{\varepsilon,\mu}[\vec{\mathbf{S}}_{lb}(x_i, y_j) - \vec{\mathbf{s}}_{lb}(x_i, y_j)]| \le C(\bar{h}_i + \bar{k}_j)\frac{\mu^3}{\varepsilon^2},$$

and using the barrier function

$$\vec{\Psi}^{\pm}(x_i, y_j) = C\left(\frac{N^{-1}\mu^2}{\varepsilon^2\ln N}(\sigma_1 - x_i) + \frac{N^{-1}\mu^2}{\varepsilon^2\ln N}(\sigma_2 - y_j)\right) \pm (\vec{\mathbf{S}}_{lb}(x_i, y_j) - \vec{\mathbf{s}}_{lb}(x_i, y_j))$$

to attain a feasible bound on the error in the layer region $\Omega^{N,N}_{1,2}$, and the discrete minimum principle on $\bar{\Omega}^{N,N}_{1,2}$, we obtain

$$|(\vec{\mathbf{s}}_{lb}(x_i, y_j) - \vec{\mathbf{S}}_{lb}(x_i, y_j))| \le CN^{-1}, \quad (x_i, y_j) \in \bar{\Omega}^{N,N}_{1,2}. \tag{4.18}$$

Then, the result follows from (4.16) and (4.18). □

Analogous results hold for the remaining corner layer components $\vec{\mathbf{s}}_{br}$, $\vec{\mathbf{s}}_{rt}$ and $\vec{\mathbf{s}}_{lt}$, which can see in the next lemma.

Lemma 4.5. *At each grid point $(x_i, y_j) \in \Omega^{N,N}$, the error estimate of the remaining corner layer components for both the cases $\alpha\mu^2 \le \lambda\varepsilon$ and $\alpha\mu^2 > \lambda\varepsilon$ are as follows:*

$$|\vec{\mathbf{s}}_{br}(x_i, y_j) - \vec{\mathbf{S}}_{br}(x_i, y_j)| \le CN^{-1},$$
$$|\vec{\mathbf{s}}_{rt}(x_i, y_j) - \vec{\mathbf{S}}_{rt}(x_i, y_j)| \le CN^{-1},$$
$$|\vec{\mathbf{s}}_{lt}(x_i, y_j) - \vec{\mathbf{S}}_{lt}(x_i, y_j)| \le CN^{-1},$$

where λ is defined in (1.3).

Then, we are in disposition to prove the main result of the work, which proves the uniform convergence of first order of the numerical method when it is defined on the Bakhvalov–Shishkin mesh.

Theorem 4.6. *Consider $\vec{\mathbf{z}}$ and $\vec{\mathbf{Z}}$ are the continuous and discrete solutions of problems (1.1)* and *(3.5), respectively, on the constructed nonuniform Bakhvalov–Shishkin mesh, assuming that (1.2) holds. Then, for both the cases $\alpha\mu^2 \le \lambda\varepsilon$ and $\alpha\mu^2 > \lambda\varepsilon$, the error at the mesh points $(x_i, y_j) \in \bar{\Omega}^{N,N}$ satisfies*

$$|\vec{\mathbf{Z}}(x_i, y_j) - \vec{\mathbf{z}}(x_i, y_j)| \le CN^{-1}.$$

Proof. Combining Lemmas 4.1, 4.2, 4.3, 4.4 and 4.5 the required result follows. □

5. Numerical experiments

We describe the implementation of the standard 5-point finite difference method with B-S-mesh in Section 3 and to illustrate the performance of the numerical method developed in the preceding sections, and focused on two examples of the type given in (1.1). These problems are solved using MATLAB R2022a on a system with 32 Gb RAM, and an i5 processor associated with 1.8 GHz. We observed that the computational time to achieve the result is relatively longer as the current problem is complex. However, the sparse matrix is being used to solve the linear system in the algorithm to reduce the computational time and the storage of the system.

To solve the test problems, we have ordered the numerical solution in the following form:

$$U = \begin{cases} U_1(x_0,y_0), U_1(x_1,y_0), \dots, U_1(x_N,y_0), \\ U_1(x_0,y_1), U_1(x_1,y_1), \dots, U_1(x_N,y_1), \\ U_1(x_0,y_2), U_1(x_1,y_2), \dots, U_1(x_N,y_2), \\ \dots\dots\dots\dots\dots\dots\dots\dots\dots\dots\dots\dots\dots \\ U_1(x_0,y_N), U_1(x_1,y_N), \dots, U_1(x_N,y_N), \\ U_2(x_0,y_0), U_2(x_1,y_0), \dots, U_2(x_N,y_0), \\ U_2(x_0,y_1), U_2(x_1,y_1), \dots, U_2(x_N,y_1), \\ \dots\dots\dots\dots\dots\dots\dots\dots\dots\dots\dots\dots\dots \\ U_2(x_0,y_N), U_2(x_1,y_N), \dots, U_2(x_N,y_N), \end{cases}$$

where $U_1(x_0,y_i)$, $U_1(x_i,y_0)$, $U_1(x_N,y_i)$ and $U_1(x_i,y_N)$, $i = 0,\dots,N$, are calculated by using the boundary conditions. Then, the resulting linear system can be written as

$$[A]_{(2(N+1)^2,2(N+1)^2)}[U]_{(2(N+1)^2,1)} = [F]_{(2(N+1)^2,1)},$$

and we solve this system by using MATLAB taking into account that the matrix A is sparse.

Example 5.1. First, we consider the two-parameter weakly-coupled system of two-dimensional boundary value problem

$$\varepsilon\left(\frac{\partial^2\vec{\mathbf{z}}}{\partial x^2} + \frac{\partial^2\vec{\mathbf{z}}}{\partial y^2}\right) + \mu\left(\vec{\mathbf{A}}(x,y)\frac{\partial\vec{\mathbf{z}}}{\partial x} + \vec{\mathbf{B}}(x,y)\frac{\partial\vec{\mathbf{z}}}{\partial y}\right) - \vec{\mathbf{C}}(x,y)\vec{\mathbf{z}} = \vec{\mathbf{f}}(x,y), \quad \forall(x,y)\in\Omega,$$

where boundary conditions as well as convection, reaction coefficients and source terms are given by

$$\vec{\mathbf{z}}(x,0) = \vec{\mathbf{z}}(x,1) = \vec{\mathbf{z}}(0,y) = \vec{\mathbf{z}}(1,y) = 0,$$
$$\vec{\mathbf{A}}(x,y) = \begin{pmatrix} 2+\exp(xy) & 0 \\ 0 & 1+\exp(xy) \end{pmatrix}, \ \vec{\mathbf{B}}(x,y) = \begin{pmatrix} 1+\exp(xy) & 0 \\ 0 & 2+\exp(xy) \end{pmatrix}, \ \vec{\mathbf{C}}(x,y) = \begin{pmatrix} 4+xy & 2+xy \\ 2+xy & 4+xy \end{pmatrix},$$
$$\vec{\mathbf{f}}(x,y) = \left(\sin(\pi xy), \cos\left(\frac{\pi}{2}xy\right)\right)^T.$$

Example 5.2. The data of the second example are given by

$$\vec{\mathbf{z}}(x,0) = \vec{\mathbf{z}}(x,1) = x(1-x),\ \vec{\mathbf{z}}(0,y) = \vec{\mathbf{z}}(1,y) = y(1-y),$$
$$\vec{\mathbf{A}}(x,y) = \begin{pmatrix} 1+x^2y^2 & 0 \\ 0 & 3-xy \end{pmatrix}, \ \vec{\mathbf{B}}(x,y) = \begin{pmatrix} 2+\sin(x+y) & 0 \\ 0 & 3-\cos(x+y) \end{pmatrix},$$
$$\vec{\mathbf{C}}(x,y) = \begin{pmatrix} 4+x+y & 3-xy \\ 3+\exp(xy) & 4-x^2y^2 \end{pmatrix}, \quad \vec{\mathbf{f}}(x,y) = \left(\cos(\pi xy/2), \sin(\pi xy)\right)^T.$$

Figs. 2, 3 and 4, 5 display the two components of the numerical solution for Examples 5.1 and 5.2, respectively, taking different values of the diffusion and the convection parameters ε and μ, and a value of the discretization parameter N. From them, we clearly observe the boundary and the internal layers in the solution.

As the exact solution of these problems is unknown, to approximate the maximum point-wise errors we use, in a usual way, the double mesh technique (see [33]). Then, we calculate

$$E^{N,N}_{\epsilon,\mu} = \max_{(x_i,y_j)\in\bar{\Omega}^{N,N}} |Z^{2N,2N}(x_{2i},y_{2j}) - Z^{N,N}(x_i,y_j)|$$

where $Z^{2N,2N}(x_{2i},y_{2j})$ is the numerical solution obtained on a mesh with $2N$ subintervals taking the mesh points of the coarse mesh and their midpoints on each direction. The parameter uniform maximum point-wise errors are determined applying the formula

$$E^{N,N} = \max_{\epsilon,\mu} E^{N,N}_{\epsilon,\mu}.$$

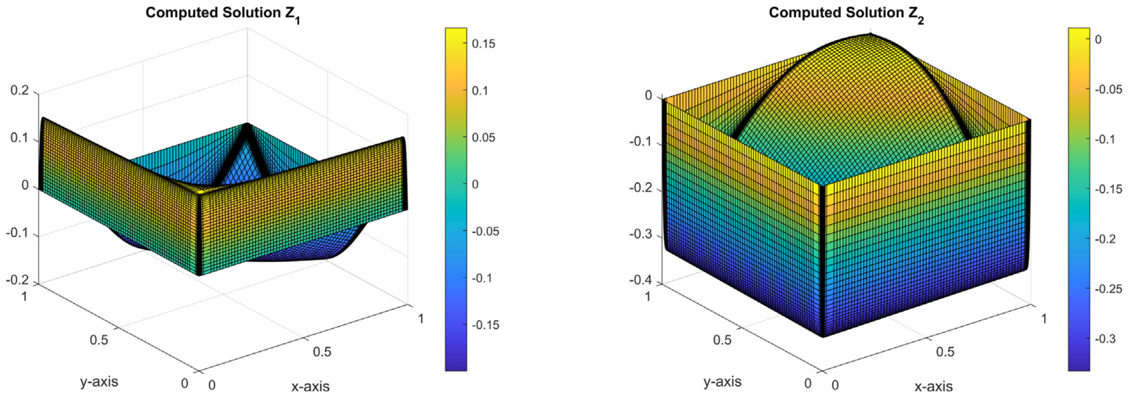

(a) Surface graph of the numerical solution z_1; (b) Surface graph of the numerical solution z_2;

Fig. 2. When $\epsilon = 10^{-5}, \mu = 10^{-7}, N = 128$ for Example 5.1.

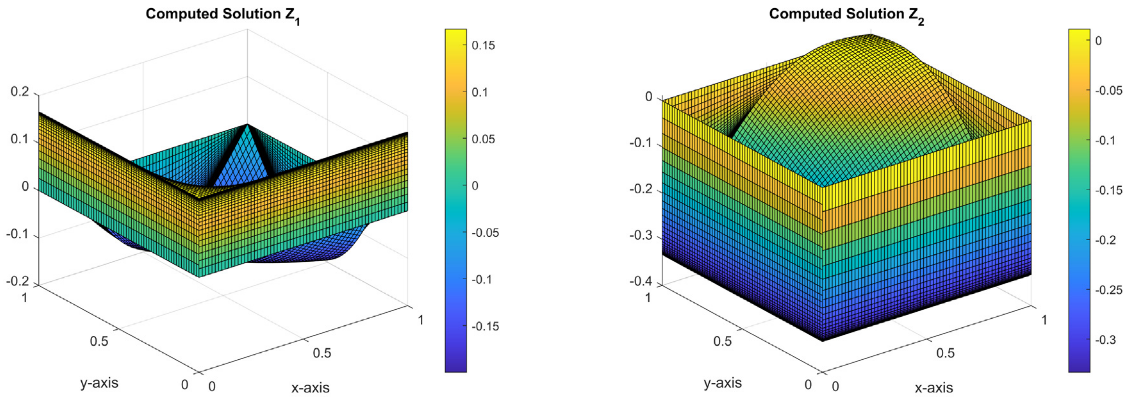

(a) Surface graph of the numerical solution z_1; (b) Surface graph of the numerical solution z_2;

Fig. 3. When $\epsilon = 10^{-16}, \mu = 10^{-7}, N = 128$ for Example 5.1.

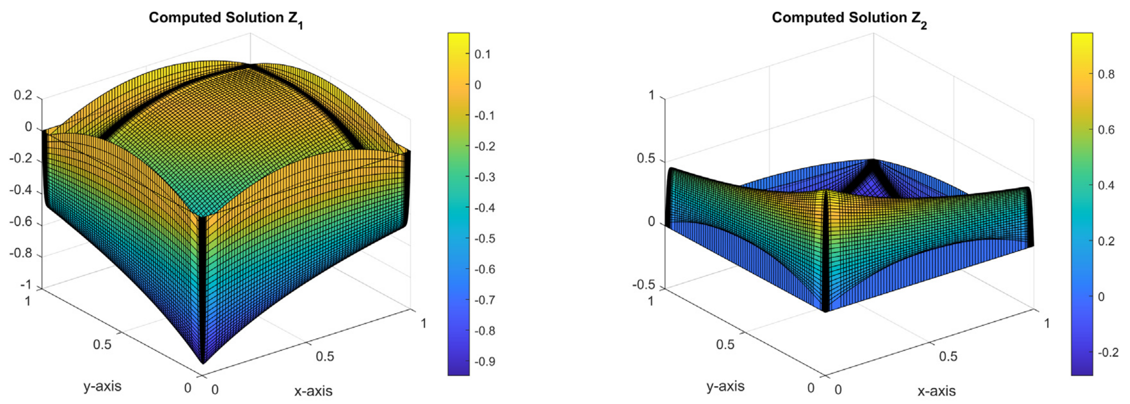

(a) Surface graph of the numerical solution z_1; (b) Surface graph of the numerical solution z_2;

Fig. 4. When $\epsilon = 10^{-5}, \mu = 10^{-7}, N = 128$ for Example 5.2.

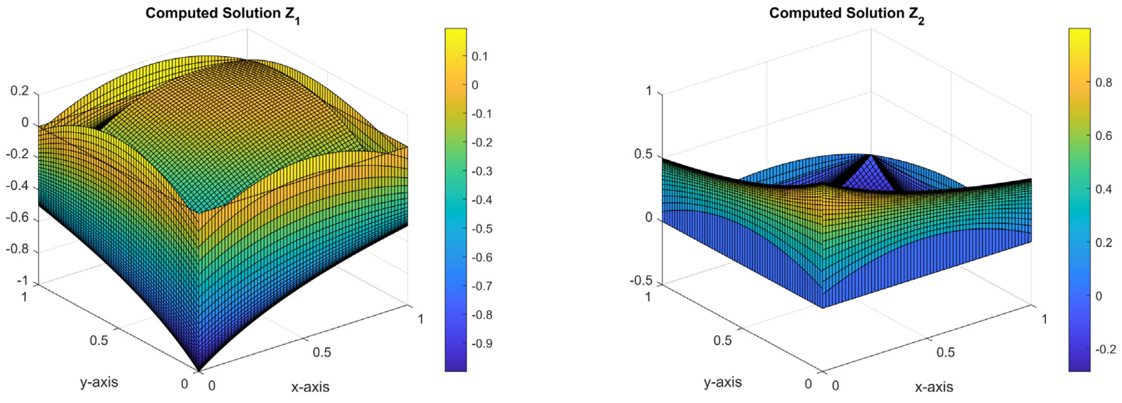

(a) Surface graph of the numerical solution z_1; (b) Surface graph of the numerical solution z_2;

Fig. 5. When $\epsilon = 10^{-16}$, $\mu = 10^{-7}$, $N = 128$ for Example 5.2.

Table 1
For Example 5.1, maximum point-wise errors $E^{N,N}$ and orders of convergence $Q^{N,N}$ calculated for z_1 using B-S-mesh.

$\mu = 1.e-7$						
ε	N = 32	N = 64	N = 128	N = 256	N = 512	N = 1024
$1.e-4$	1.330e−3	3.923e−4	1.069e−4	2.823e−5	7.274e−6	5.259e−6
$1.e-6$	1.340e−3	3.929e−4	1.070e−4	2.821e−5	7.260e−6	1.847e−6
$1e-8$	1.335e−3	3.896e−4	1.060e−4	2.779e−5	7.115e−6	1.804e−6
$1.e-10$	1.265e−3	3.545e−4	9.480e−5	2.942e−5	1.182e−5	5.199e−6
$1.e-12$	1.861e−3	8.383e−4	3.756e−4	1.762e−4	8.515e−5	4.183e−5
$1.e-14$	8.366e−3	5.141e−3	2.858e−3	1.510e−3	7.762e−4	3.936e−4
$1.e-16$	1.379e−2	8.224e−3	4.501e−3	2.369e−3	1.216e−3	6.164e−4
$1.e-18$	1.383e−2	8.241e−3	4.510e−3	2.374e−3	1.218e−3	6.175e−4
$1.e-20$	1.383e−2	8.241e−3	4.510e−3	2.374e−3	1.218e−3	6.175e−4
$1.e-22$	1.383e−2	8.241e−3	4.510e−3	2.374e−3	1.218e−3	6.175e−4
$1.e-24$	1.383e−2	8.241e−3	4.510e−3	2.374e−3	1.218e−3	6.175e−4
$E^{N,N}$	1.383e−2	8.241e−3	4.510e−3	2.374e−3	1.218e−3	6.175e−4
$Q^{N,N}$	0.7469	0.8697	0.9258	0.9628	0.9800	–

Using the previous values, the uniform numerical orders of convergence are given by

$$Q^{N,N} = \log_2\left(\frac{E^{N,N}}{E^{2N,2N}}\right).$$

Tables 1, 2 5, 6 show the maximum errors and the uniform orders of convergence for Examples 5.1 and 5.2, respectively, for the first component, and Tables 3, 4 7, 8 the corresponding ones for the second component, using the B-S mesh; from them, we clearly see the first order of uniform convergence of the numerical method. So, the numerical results are according with the theoretical result proved in Theorem 4.6. In Tables 9, and 10, we show the comparison between the maximum point-wise errors and the order of convergence using S-mesh and B-S-mesh for Examples 5.1 and 5.2, respectively; from these two tables, we observe that the use of the Bakhvalov–Shishkin mesh gives better results than the corresponding ones when the Shishkin mesh is used, something that is usual in the numerical resolution of singularly perturbed problems.

6. Conclusions

This work is concerned with a two-parameter weakly-coupled elliptic system of singularly perturbed 2-D convection–reaction–diffusion problems. A finite-difference scheme with layer-adapted nonuniform Bakhvalov–Shishkin mesh that yields first-order of uniform convergence, is used to generate a parameter-uniform discrete solution. The analytical and the discrete solutions are split into a sum of smooth, boundary and corner components to address the convergence analysis and to obtain appropriate bounds for the error. The numerical experiments, for two test problems, show that the numerical results corroborate in the practice the theoretical analysis.

Table 2
For Example 5.1, maximum point-wise errors $E^{N,N}$ and orders of convergence $Q^{N,N}$ calculated for z_1 using B-S-mesh.

$\mu = 1.e-4$						
ε	N = 32	N = 64	N = 128	N = 256	N = 512	N = 1024
$1.e-4$	1.251e−3	3.532e−4	9.442e−5	2.955e−5	1.189e−5	6.576e−6
$1.e-6$	1.864e−3	8.392e−4	3.759e−4	1.764e−4	8.525e−5	4.187e−5
$1.e-8$	8.366e−3	5.141e−3	2.858e−3	1.510e−3	7.762e−4	3.936e−4
$1.e-10$	1.379e−2	8.224e−3	4.501e−3	2.369e−3	1.216e−3	6.164e−4
$1.e-12$	1.383e−2	8.241e−3	4.510e−3	2.374e−3	1.218e−3	6.175e−4
$1.e-14$	1.383e−2	8.241e−3	4.510e−3	2.374e−3	1.218e−3	6.175e−4
$1.e-16$	1.383e−2	8.241e−3	4.510e−3	2.374e−3	1.218e−3	6.175e−4
$1.e-18$	1.383e−2	8.241e−3	4.510e−3	2.374e−3	1.218e−3	6.175e−4
$1.e-20$	1.383e−2	8.241e−3	4.510e−3	2.374e−3	1.218e−3	6.175e−4
$1.e-22$	1.383e−2	8.241e−3	4.510e−3	2.374e−3	1.218e−3	6.175e−4
$1.e-24$	1.383e−2	8.241e−3	4.510e−3	2.374e−3	1.218e−3	6.175e−4
$E^{N,N}$	1.383e−2	8.241e−3	4.510e−3	2.374e−3	1.218e−3	6.175e−4
$Q^{N,N}$	0.7469	0.8697	0.9258	0.9628	0.9800	–

Table 3
For Example 5.1, maximum point-wise errors $E^{N,N}$ and orders of convergence $Q^{N,N}$ calculated for z_2 using B-S-mesh.

$\mu = 1.e-7$						
ε	N = 32	N = 64	N = 128	N = 256	N = 512	N = 1024
$1.e-4$	1.345e−3	3.993e−4	1.081e−4	2.836e−5	7.292e−6	4.600e−6
$1.e-6$	1.356e−3	3.999e−4	1.080e−4	2.833e−5	7.278e−6	1.849e−6
$1.e-8$	1.350e−3	3.965e−4	1.067e−4	2.791e−5	7.132e−6	1.806e−6
$1.e-10$	1.277e−3	3.596e−4	9.529e−5	3.038e−5	1.365e−5	6.665e−6
$1.e-12$	2.170e−3	1.021e−3	5.019e−4	2.489e−4	1.239e−4	6.183e−5
$1.e-14$	1.382e−2	8.497e−3	4.733e−3	2.505e−3	1.290e−3	6.543e−4
$1.e-16$	2.716e−2	1.625e−2	8.916e−3	4.696e−3	2.411e−3	1.223e−3
$1.e-18$	2.765e−2	1.648e−2	9.020e−3	4.747e−3	2.436e−3	1.235e−3
$1.e-20$	2.766e−2	1.648e−2	9.021e−3	4.747e−3	2.437e−3	1.235e−3
$1.e-22$	2.766e−2	1.648e−2	9.021e−3	4.747e−3	2.437e−3	1.235e−3
$1.e-24$	2.766e−2	1.648e−2	9.021e−3	4.747e−3	2.437e−3	1.235e−3
$E^{N,N}$	2.766e−2	1.648e−2	9.021e−3	4.747e−3	2.437e−3	1.235e−3
$Q^{N,N}$	0.7471	0.8694	0.9263	0.9619	0.9806	–

Table 4
For Example 5.1, maximum point-wise errors $E^{N,N}$ and orders of convergence $Q^{N,N}$ calculated for z_2 using B-S-mesh.

$\mu = 1.e-4$						
ε	N = 32	N = 64	N = 128	N = 256	N = 512	N = 1024
$1.e-4$	1.263e−3	3.583e−4	9.490e−5	2.965e−5	1.352e−5	6.748e−6
$1.e-6$	2.165e−3	1.020e−3	5.011e−4	2.484e−4	1.237e−4	6.171e−5
$1.e-8$	1.382e−2	8.497e−3	4.733e−3	2.505e−3	1.290e−3	6.543e−4
$1.e-10$	2.716e−2	1.625e−2	8.916e−3	4.696e−3	2.411e−3	1.223e−3
$1.e-12$	2.765e−2	1.648e−2	9.020e−3	4.747e−3	2.436e−3	1.235e−3
$1.e-16$	2.766e−2	1.648e−2	9.021e−3	4.747e−3	2.437e−3	1.235e−3
$1.e-18$	2.766e−2	1.648e−2	9.021e−3	4.747e−3	2.437e−3	1.235e−3
$1.e-20$	2.766e−2	1.648e−2	9.021e−3	4.747e−3	2.437e−3	1.235e−3
$1.e-22$	2.766e−2	1.648e−2	9.021e−3	4.747e−3	2.437e−3	1.235e−3
$1.e-24$	2.766e−2	1.648e−2	9.021e−3	4.747e−3	2.437e−3	1.235e−3
$E^{N,N}$	2.766e−2	1.648e−2	9.021e−3	4.747e−3	2.437e−3	1.235e−3
$Q^{N,N}$	0.7471	0.8694	0.9263	0.9619	0.9806	–

Table 5
For Example 5.2, maximum point-wise errors $E^{N,N}$ and orders of convergence $Q^{N,N}$ calculated for z_1 using B-S-mesh.

$\mu = 1.e-7$						
ε	N = 32	N = 64	N = 128	N = 256	N = 512	N = 1024
$1.e-4$	1.033e−2	3.872e−3	1.345e−3	4.444e−4	1.396e−4	4.135e−5
$1.e-6$	1.150e−2	4.597e−3	1.730e−3	6.331e−4	2.285e−4	8.185e−5
$1.e-8$	1.157e−2	4.652e−3	1.766e−3	6.531e−4	2.383e−4	8.634e−5
$1.e-10$	1.092e−2	4.328e−3	1.620e−3	5.917e−4	2.135e−4	7.651e−5
$1.e-12$	7.127e−3	2.556e−3	1.313e−3	8.004e−4	4.406e−4	2.310e−4
$1.e-14$	4.816e−2	2.944e−2	1.627e−2	8.548e−3	4.385e−3	2.221e−3
$1.e-16$	6.641e−2	4.058e−2	2.247e−2	1.180e−2	6.039e−3	3.052e−3
$1.e-18$	6.844e−2	4.236e−2	2.361e−2	1.243e−2	6.436e−3	3.388e−3
$1.e-20$	6.847e−2	4.239e−2	2.363e−2	1.244e−2	6.445e−3	3.393e−3
$1.e-22$	6.847e−2	4.239e−2	2.363e−2	1.244e−2	6.445e−3	3.393e−3
$1.e-24$	6.847e−2	4.239e−2	2.363e−2	1.244e−2	6.445e−3	3.393e−3
$E^{N,N}$	6.847e−2	4.239e−2	2.363e−2	1.244e−2	6.445e−3	3.393e−3
$Q^{N,N}$	0.6917	0.8431	0.9256	0.9487	0.9256	–

Table 6
For Example 5.2, maximum point-wise errors $E^{N,N}$ and orders of convergence $Q^{N,N}$ calculated for z_1 using B-S-mesh.

$\varepsilon = 1.e-5$						
μ	N = 32	N = 64	N = 128	N = 256	N = 512	N = 1024
$1.e-4$	8.993e−3	3.330e−3	1.164e−3	3.981e−4	1.359e−4	6.312e−5
$1.e-6$	1.118e−2	4.390e−3	1.619e−3	5.790e−4	2.033e−4	7.041e−5
$1.e-8$	1.120e−2	4.401e−3	1.624e−3	5.810e−4	2.041e−4	7.069e−5
$1.e-10$	1.120e−2	4.401e−3	1.624e−3	5.810e−4	2.041e−4	7.069e−5
$1.e-12$	1.120e−2	4.401e−3	1.624e−3	5.810e−4	2.041e−4	7.069e−5
$1.e-14$	1.120e−2	4.401e−3	1.624e−3	5.810e−4	2.041e−4	7.069e−5
$1.e-16$	1.120e−2	4.401e−3	1.624e−3	5.810e−4	2.041e−4	7.069e−5
$1.e-18$	1.120e−2	4.401e−3	1.624e−3	5.810e−4	2.041e−4	7.069e−5
$1.e-20$	1.120e−2	4.401e−3	1.624e−3	5.810e−4	2.041e−4	7.069e−5
$1.e-22$	1.120e−2	4.401e−3	1.624e−3	5.810e−4	2.041e−4	7.069e−5
$1.e-24$	1.120e−2	4.401e−3	1.624e−3	5.810e−4	2.041e−4	7.069e−5
$E^{N,N}$	1.120e−2	4.401e−3	1.624e−3	5.810e−4	2.041e−4	7.069e−5
$Q^{N,N}$	1.3476	1.4383	1.4829	1.5093	1.5297	–

Table 7
For Example 5.2, maximum point-wise errors $E^{N,N}$ and orders of convergence $Q^{N,N}$ calculated for z_2 using B-S-mesh.

$\mu = 1.e-7$						
ε	N = 32	N = 64	N = 128	N = 256	N = 512	N = 1024
$1.e-4$	1.206e−2	4.540e−3	1.584e−3	5.259e−4	1.660e−4	4.772e−5
$1.e-6$	1.330e−2	5.317e−3	2.001e−3	7.327e−4	2.646e−4	9.480e−5
$1.e-8$	1.336e−2	5.372e−3	2.039e−3	7.541e−4	2.752e−4	9.971e−5
$1.e-10$	1.259e−2	4.987e−3	1.867e−3	6.818e−4	2.459e−4	8.815e−5
$1.e-12$	9.096e−3	3.401e−3	1.616e−3	9.770e−4	5.353e−4	2.800e−4
$1.e-14$	6.081e−2	3.731e−2	2.083e−2	1.102e−2	5.673e−3	2.879e−3
$1.e-16$	8.316e−2	4.972e−2	2.725e−2	1.434e−2	7.357e−3	3.727e−3
$1.e-18$	8.298e−2	4.945e−2	2.706e−2	1.424e−2	7.311e−3	3.705e−3
$1.e-20$	8.298e−2	4.945e−2	2.706e−2	1.424e−2	7.310e−3	3.705e−3
$1.e-22$	8.298e−2	4.945e−2	2.706e−2	1.424e−2	7.310e−3	3.705e−3
$1.e-24$	8.298e−2	4.945e−2	2.706e−2	1.424e−2	7.310e−3	3.705e−3
$E^{N,N}$	8.316e−2	4.972e−2	2.725e−2	1.434e−2	7.357e−3	3.727e−3
$Q^{N,N}$	0.7421	0.8676	0.9262	0.9629	0.9811	–

Table 8
For Example 5.2, maximum point-wise errors $E^{N,N}$ and orders of convergence $Q^{N,N}$ calculated for z_2 using B-S-mesh.

$\varepsilon = 1.e-5$						
μ	N = 32	N = 64	N = 128	N = 256	N = 512	N = 1024
1.e − 4	1.034e−2	3.833e−3	1.342e−3	4.595e−4	1.572e−4	7.698e−5
1.e − 6	1.296e−2	5.092e−3	1.880e−3	6.734e−4	2.368e−4	8.211e−5
1.e − 8	1.298e−2	5.106e−3	1.886e−3	6.758e−4	2.378e−4	8.244e−5
1.e − 10	1.298e−2	5.106e−3	1.886e−3	6.759e−4	2.378e−4	8.245e−5
1.e − 12	1.298e−2	5.106e−3	1.886e−3	6.759e−4	2.378e−4	8.245e−5
1.e − 14	1.298e−2	5.106e−3	1.886e−3	6.759e−4	2.378e−4	8.245e−5
1.e − 16	1.298e−2	5.106e−3	1.886e−3	6.759e−4	2.378e−4	8.245e−5
1.e − 18	1.298e−2	5.106e−3	1.886e−3	6.759e−4	2.378e−4	8.245e−5
1.e − 20	1.298e−2	5.106e−3	1.886e−3	6.759e−4	2.378e−4	8.245e−5
1.e − 22	1.298e−2	5.106e−3	1.886e−3	6.759e−4	2.378e−4	8.245e−5
1.e − 24	1.298e−2	5.106e−3	1.886e−3	6.759e−4	2.378e−4	8.245e−5
$E^{N,N}$	1.298e−2	5.106e−3	1.886e−3	6.759e−4	2.378e−4	8.245e−5
$Q^{N,N}$	1.3460	1.4369	1.4804	1.5071	1.5282	–

Table 9
For Example 5.1 maximum point-wise errors $E^{N,N}$ and orders of convergence $Q^{N,N}$, using the B-S-mesh and S-mesh.

N	First Component z_1				Second Component z_2			
	B-S-mesh		S-mesh		B-S-mesh		S-mesh	
	$E^{N,N}$	$Q^{N,N}$	$E^{N,N}$	$Q^{N,N}$	$E^{N,N}$	$Q^{N,N}$	$E^{N,N}$	$Q^{N,N}$
32	1.383e−2	0.7469	2.473e−2	0.1648	2.766e−2	0.7471	4.946e−2	0.1648
64	8.241e−3	0.8697	2.206e−2	0.3582	1.648e−2	0.8694	4.412e−2	0.3578
128	4.510e−3	0.9258	1.721e−2	0.4976	9.021e−3	0.9263	3.443e−2	0.4974
256	2.374e−3	0.9628	1.219e−2	0.5872	4.747e−3	0.9619	2.439e−2	0.5876
512	1.218e−3	0.9800	8.114e−3	0.6830	2.437e−3	0.9806	1.623e−2	0.6829
1024	6.175e−4	–	5.054e−3	–	1.235e−3	–	1.011e−2	–

Table 10
For Example 5.2, maximum point-wise errors $E^{N,N}$ and orders of convergence $Q^{N,N}$, using the B-S-mesh and S-mesh.

N	First Component z_1				Second Component z_2			
	B-S-mesh		S-mesh		B-S-mesh		S-mesh	
	$E^{N,N}$	$Q^{N,N}$	$E^{N,N}$	$Q^{N,N}$	$E^{N,N}$	$Q^{N,N}$	$E^{N,N}$	$Q^{N,N}$
32	1.120e−2	1.3476	3.187e−2	0.9603	1.298e−2	1.3460	2.974e−2	1.0443
64	4.401e−3	1.4383	1.638e−2	0.7226	5.106e−3	1.4369	1.442e−2	0.5023
128	1.624e−3	1.4829	9.926e−3	1.2367	1.886e−3	1.4804	1.018e−2	1.1583
256	5.810e−4	1.5093	4.212e−3	1.3468	6.759e−4	1.5071	4.561e−3	1.4078
512	2.041e−4	1.5297	1.656e−3	1.3342	2.378e−4	1.5282	1.719e−3	1.4304
1024	7.069e−5	–	6.568e−4	–	8.245e−5	–	6.378e−4	–

Data availability

No data was used for the research described in the article.

Acknowledgments

The authors thank to the referees for their valuable suggestions which have helped to improve the presentation of this paper.

Funding

The research of first author was partially supported by the project MTM2017-83490-P, the Aragón Government and European Social Fund (group E24-17R) and the Public University of Navarre, Spain. The second author wishes to thank Ministry of Education (MoE), Govt. of India for their financial support.

References

[1] G. Barenblatt, I. Zheltov, L. Kochin, Basic concepts in the theory of seepage of homogeneous liquids in fissured rocks, J. Appl. Math. and Mech. 24 (1960) 1286–1303.
[2] I. Epstein, L. Lengyel, S. Kádár, M. Kagan, M. Yokoyama, New systems for pattern formation studies, Physica A 188 (1992) 26–33.

[3] Y. Kan-On, M. Mimura, Singular perturbation approach to a 3-component reaction-diffusion system arising in population dynamics, SIAM J. Math. Anal. 29 (1998) 1519–1536.
[4] C. Pao, Nonlinear Parabolic and Elliptic Equations, Plenum Press, 1992.
[5] G. Thomas, Towards an improved turbulence model for wave-current interactions, Tech. rep, 2nd Annual Report to EU MAST-III Project The Kinematics and Dynamics of Wave-Current Interactions, 1998.
[6] J. Gracia, E. O'Riordan, M. Pickett, A parameter robust second order numerical method for a singularly perturbed two-parameter problem, Appli. Numer. Math. 56 (7) (2005) 962–980.
[7] E. O'Riordan, M. Pickett, G. Shishkin, Numerical methods for singularly perturbed elliptic problems containing two perturbation parameters, Mathematical Modelling and Analysis 11 (2) (2006) 199–212.
[8] L. Govindarao, J. Mohapatra, S. Sahu, Uniformly convergent numerical method for singularly perturbed two parameter time delay parabolic problem, Int. J. Appl. Comput. Math. 5:91 (2019) http://dx.doi.org/10.1007/s40819-019-0672-5.
[9] L. Govindarao, S. Sahu, J. Mohapatra, Uniformly convergent numerical method for singularly perturbed two parameter time delay parabolic problem with two small parameters, Iran. J. Sci. Technol. Trans. A: Sci. 43 (2019) 2373–2383.
[10] S. Priyadarshana, J. Mohapatra, S. Pattaniak, Parameter uniform optimmal order numerical approximations for time-delayed parabolic convection diffusion problems involving two small parameters, Comput. Appl. Math. 41:233 (2022) http://dx.doi.org/10.1007/s40314-022-01928-w.
[11] S. Bellew, E. O'Riordan, A parameter robust numerical method for a system of two singularly convection-diffusion equations, Appl. Numer. Math. 51 (2004) 171–186.
[12] Z. Cen, Parameter-uniform finite difference scheme for a system of coupled singularly perturbed convection-diffusion equations, J. Syst. Sci. Complex. 18 (4) (2005) 498–510.
[13] T. Linss, Analysis of an upwind finite-difference scheme for a system of coupled singularly perturbed convection-diffusion equations, Computing 79 (2007) 23–32.
[14] R. Priyadharshini, N. Ramanujam, A. Tamilsevan, Hybrid difference schemes for a system of singularly perturbed convection-diffusion equations, J. Appl. Math. Inf. 27 (2009) 1001–1015.
[15] R. Kellogg, T. Linss, M. Stynes, A finite difference method on layer-adapted meshes for an elliptic reaction-diffusion system in two dimensions, Math. Comp. 774 (2008) 2085–2096.
[16] T. Linss, M. Stynes, Numerical solution of systems of singularly perturbed differential equations, Comput. Methods Appl. Math. 5 (2009) 165–191.
[17] C. Clavero, J. Jorge, A splitting uniformly convergent method for one-dimensional parabolic singularly perturbed convection-diffusion systems, Appl. Numer. Math. 183 (2023) 317–332.
[18] L. Liu, G. Long, Y. Zhang, Parameter uniform numerical method for a system of two coupled singularly perturbed parabolic convection-diffusion equations, Adv. Differential Equations 2018 (450) (2018) http://dx.doi.org/10.1186/s13662--018-1907-13.
[19] M. Singh, S. Natesan, Numerical analysis of singularly perturbed system of parabolic convection-diffusion problem with regular boundary layers, Diff. Equat. Dyn. Syst. (2019) http://dx.doi.org/10.1007/s12591-019-00462-2.
[20] M. Singh, S. Natesan, A parameter-uniform hybrid finite difference schme for singularly perturbed system of parabolic convection-diffusion problems, Int. J. Comput. Math. 97 (4) (2020) 875–903.
[21] C. Clavero, J. Jorge, An efficient numerical method for singularly perturbed time dependent parabolic 2D convection-diffusion systems, J. Comput. Appl. Math. 354 (2019) 431–444.
[22] M. Singh, S. Natesan, A robust computational method for singularly perurbed system of 2D parabolic convection-diffusion problems, Int. J. Math. Model. Numer. Optim. 9 (2) (2019) 127–157.
[23] K. Aarthika, V. Shanthi, H. Ramos, A computational approach for a two-parameter singularly perturbed system of partial differential equations with discontinuous coefficients, Appl. Math. Comput. 434 (2022) 127409.
[24] O.A. Ladyzhenskaya, N.N. Ural'tseva, Linear and Quasilinear Elliptic Equations, 1968,
[25] H. Han, R. Kellogg, Differentiability properties of solutions of the equation $-\varepsilon^2 \Delta u + ru = f(x, y)$ in a square, SIAM J. Math. Anal. 21 (2) (1990) 394–408.
[26] C. Clavero, J. Gracia, E. O'Riordan, A parameter robust numerical method for a two dimensional reaction-diffusion problem, Math. of Comp. 74 (2) (2005) 1743–1758.
[27] J. Miller, E. O'Riordan, G. Shishkin, L.P. Shishkina, Fitted mesh methods for problems with parabolic boundary layers, Math. Proc. R. Ir. Acad. 98A (1998).
[28] E. O'Riordan, M. Pickett, G. Shishkin, Numerical methods for singularly perturbed elliptic problems containing two perturbation parameters, Math. Model. Anal. 11 (2) (2006) 199–212.
[29] E. O'Riordan, M. Pickett, A parameter-uniform numerical method for a singularly perturbed two parameter elliptic problem, Adv. Comput. Math. 35 (1) (2011) 57–82.
[30] T. Linß, Layer-Adapted Meshes for Reaction-Convection-Diffusion Problems, Springer, 2009.
[31] H. Roos, T. Linß, Sufficient conditions for uniform convergence on layer-adapted grids, Computing 63 (1) (1999) 27–45.
[32] K. Aarthika, R. Shiromani, V. Shanthi, A higher-order finite difference method for two-dimensional singularly perturbed reaction-diffusion with source-term-discontinuous problem, Comput. Math. Appl. 118 (2022) 56–73.
[33] P. Farrell, A. Hegarty, J. Miller, E. O'Riordan, G. Shishkin, Robust Computational Techniques for Boundary Layers, CRC Press, 2000.